Characterization of C8Orf88: A Novel eIF4E-Binding Protein

Lauren Pugsley

Department of Biochemistry

McGill University, Montreal

April 2022

A thesis submitted to McGill University in partial fulfillment of the requirements of the degree of Master of Science.

DEDICATION

I dedicate this work to my family and my friends, who’s support has been invaluable throughout my studies.

ABSTRACT

Translation initiation is the most tightly regulated step in protein synthesis. Cap-dependent translation is most commonly used by eukaryotic cells under normal conditions, and this process begins by recruitment of the eukaryotic initiation factor (eIF) 4F complex to the 5’ cap structure of mRNAs. The eIF4F complex is composed of the DEAD-box helicase eIF4A, the large scaffolding protein eIF4G, and the cap-binding protein eIF4E. The rate-limiting factor in eIF4F complex formation is eIF4E, and as such its availability determines the rates of translation initiation and ultimately the rates of protein synthesis. Additionally, eIF4E is a recognized proto-oncogene and its overexpression has been documented in many malignancies. A central mechanism in the regulation of eIF4E availability is sequestration by eIF4E-binding proteins (4EBPs). 4EBPs are phosphoproteins and targets of mTORC1. Upon phosphorylation by active mTORC1, the 4EBPs lose their affinity for eIF4E and release it for formation of the eIF4F complex, increasing rates of translation initiation. Here, we characterize a protein called C8Orf88 as a novel 4EBP. Using Northern blot analysis and RT-qPCR, we determine expression of C8Orf88 to be testis-specific. Furthermore, we validate the interaction between C8Orf88 and eIF4E both *in vitro* and in cells. Identification of a novel testis-specific 4EBP emphasizes the evolutionarily conserved mechanisms that regulate translation initiation, and we speculate C8Orf88’s potential relevance in the physiology and malignancies of its associated tissue type.

RÉSUMÉ

L'initiation de la traduction est l'étape de la synthèse des protéines la plus hautement régulé. Sous conditions normales, la traduction est dépendante sur la structure « cap » près du bout 5' de l'ARNm. Ce processus commence avec le recrutement d'un complexe de trois facteurs d'initiation nommée eIF4F. Il est composé de trois sous unités : la protéine hélicase à motif DEAD-box eIF4A (« *eukaryotic Initiation Factor 4A* »), la grande protéine échafaudage eIF4G (*« eukaryotic Initiation Factor 4G »*), et la protéine s'attachant au structure « cap » de l'ARNm eIF4E (*« eukaryotic Initiation Factor 4E »*). Le facteur limitant du complexe eIF4F est eIF4E, et ainsi sa disponibilité détermine les taux de traduction et finalement les taux de synthèse protéique. De plus, eIF4E est reconnu comme « proto-oncogene » et sa surexpression a été documenté dans un nombre de cancers. Une manière par laquelle les niveaux de eIF4E sont gérer est par piégeage par des protéines nommées 4EBPs (« *eIF4E-binding protein* »), qui séquestrent eIF4E. Les 4EBPs sont une famille de phosphoprotéines cibler par mTORC1. Une fois phosphoryler par mTORC1, les 4EBPs subit une perte d'affinité pour eIF4E qui est ensuite libérer pour joindre la complexe eIF4F, dirigeant une hausse de taux de synthèse protéique. Ici, on caractérise une nouvelle protéine 4EBP nommée C8Orf88. En utilisant une analyse Northern et la PCR quantitative-transcription inverse, on détermine que C8Orf88 est une protéine testiculaire. De plus, on confirme l'interaction entre eIF4E et C8Orf88 *in vitro* et en cellules. L'identification d'une nouvelle protéine 4EBP particulier au testicule fait ressortir l'importance de la régulation de la synthèse protéique conservée au cours de l'évolution. On prépose que C8Orf88 peut avoir des implications dans la physiologie et les malignités testiculaires.

ACKNOWLEDGEMENTS

It would not be right to thank anyone other than Dr. Jerry Pelletier first. Jerry has taught me more than he will know both about science and life. His character and resilience are admirable, and I thank him for being a constant mentor and role model. He provides me and everyone in our lab with every resource and guidance needed to do what we're passionate about, and we are all lucky to be supported by him.

I would also like to thank all the members of the lab, past and present. Firstly Dr. Regina Cencic, for teaching me nearly every technical skill I know and who has mentored me since my days as a confused undergraduate student. Dr. Francis Robert, for being generous with his time and for always giving me new perspectives on my project. Patrick Sénéchal, for fixing all our problems and working magic to keep the lab stocked during the pandemic-induced material shortages. Samer Girgis, for his thoughtful insights about science, running and life. Sai Kiran Naineni, for his attentive ideas in lab meetings and his dance moves, out of lab meetings. Kesha Patel, for being my bench mate, chat mate and sharer of equipment. Jordan Scott-Talib, for his generosity and good taste in music. Leo Shen, for taking time to teach me what he knew, for trusting me with his project and for being a friend. Jennifer Chu, for being an admirable scientist and baker who I am lucky to have met. Minza Haque, for her inquisitiveness and spunk. Finally, Sofia Moranis, for always keeping the lab running smoothly, and well-decorated on holidays.

My Research Advisory Committee, Dr. Jose Teodoro and Dr. Nahum Sonenberg, have also been generous with their time and I'm humbled to have been able to discuss my project with them. I thank them for their thorough questions and insight.

Lastly, I would like to thank the Canadian Institutes of Health Research (CIHR), Défi Canderel, the Goodman Cancer Institute, and the Department of Biochemistry for funding my studies.

It bewilders me how much I have learned during my time in the Pelletier lab, and I thank everyone who has gifted me their time, knowledge, and support from the bottom of my heart.

TABLE OF CONTENTS

LIST OF FIGURES

LIST OF TABLES

ABBREVIATIONS

4EBP	eIF4E-Binding Protein
4EHP	eIF4E-Homology Protein
4EBM	eIF4E-Binding Motif
AML	Acute Myeloid Leukemia
ARCA	Anti-Reverse Cap Analog
ASD	Autism Spectrum Disorder
ATP	Adenosine Triphosphate
BFDR	Bayesian False Discovery Rate
BGSS	Bovine Growth Supplemented Serum
BioID	Proximity-dependent Biotin Identification
cDNA	Complementary DNA
CREF	Cloned Rat Embryonic Fibroblast
Ct	Cycle threshold
CYR61	Cysteine-rich angiogenic inducer 61
DAPI	4',6-diamidino-2-phenylindole
DDF	Differential Detergent Fractionation
DMEM	Dulbecco's Modified Eagle's Medium
EDTA	Ethylenediaminetetraacetic acid
eEF2	Eukaryotic Elongation Factor 2
EGTA	Ethylene glycol tetraacetic acid
eIF	Eukaryotic Initiation Factor
EMCV	Encephalomyocarditis
ERK	Extracellular-signal-Regulated Kinase
E1A	Early region 1A
GAPDH	Glyceraldehyde-3-phosphate dehydrogenase
GCT	Germ Cell Tumor
GO	Gene Ontology
GST	Glutathione S-transferase
GTP	Guanosine Triphosphate
HES1	Hairy and Enhancer of Split-1
hnRNPA/B	Heterogeneous nuclear Ribonucleoprotein A/B
HRP	Horseradish Peroxidase
IHC	Immunohistochemistry
IP	Immunoprecipitation
IPTG	Isopropylthio-β-galactosidase
IRES	Internal Ribosome Entry Site

ITAF	IRES-Trans Acting Factor
MAPK	Mitogen-Activated Protein Kinase
MCL1	Myeloid Cell Leukemia 1
MEK	Mitogen-activated Extracellular signal-regulated Kinase
miRNA	MicroRNA
MMP3	Matrix Metalloproteinase 3
MMP13	Matrix Metalloproteinase 13
MNK	MAP Kinase-Interacting Kinase
mRNA	Messenger RNA
mRNP	Messenger Ribonucleoprotein
mTOR	Mechanistic/Mammalian Target of Rapamycin
mTORC1	Mechanistic/Mammalian Target of Rapamycin Complex 1
mTORC2	Mechanistic/Mammalian Target of Rapamycin Complex 2
m^7G	7-methylguanosine
m^7GTP	7-methylguanosine triphosphate
NC-loop	Non-Canonical loop
NHL	Non-Hodgkin Lymphoma
ODC	Ornithine Decarboxylase
PABP	Poly(A)-Binding Protein
PBS	Phosphate-buffered saline
PCR	Polymerase Chain Reaction
PDCD4	Programmed Cell Death Protein 4
PDGF	Platelet-Derived Growth Factor
PEI	Polyethylenimine
PIC	Pre-Initiation Complex
PI3K	Phosphoinositide 3-Kinase
PMSF	Phenylmethylsulfonyl fluoride
PVDF	Polyvinylidene fluoride
RAS	Reticular Activating System
RBD	RNA-Binding Domain
RecA	Recombinase A
RNAseq	RNA sequencing
RIPA	Radio-Immunoprecipitation Assay
RPMK	Reads Per Kilobase Million
rpS6	Ribosomal Protein S6
rRNA	Ribosomal RNA
RT-qPCR	Reverse Transcription Quantitative Polymerase Chain Reaction
SDS	Sodium dodecyl sulfate
SDS-PAGE	Sodium dodecyl sulfate Polyacrylamide Gel Electrophoresis
shRNA	Short Hairpin RNA

smFISH	Single-Molecule-Resolution *in situ* Hybridization
ssRNA	Single-stranded RNA
S6K	S6 Kinase
TBS	Tris-Buffered Saline
$tRNA_i^{Met}$	Initiator Methionyl Transfer RNA
UTR	Untranslated Region
UV	Ultraviolet
VEGF	Vascular Endothelial Growth Factor

PREFACE

This is a traditional monograph style thesis.

INTRODUCTION

Protein Synthesis

Protein synthesis is the translation of genetic information stored as mRNA into proteins, which exert their effects across all facets of a cell's biology. This orchestral process is central to all aspects of metabolism and is a key step in the regulation of gene expression(1). Protein synthesis is the most energetically demanding process undertaken by cells(2) and occurs in four steps: initiation, elongation, termination and ribosome recycling(3). Given its taxing energetic demands and fundamental role in all aspects of cell biology, this process is heavily regulated. This regulation occurs primarily at the step of translation initiation, the most intricate step in protein synthesis(3). This is in part due to the ability of cells to respond rapidly to changes in the environment. Cells maintain mRNAs that are not immediately translated but allow for rapid protein production upon stimulation; this is much faster than a transcriptional response and regulation at this level allows for a much more dynamic response(4).

Aberrant protein synthesis, particularly translation initiation, is associated with metabolic syndromes such as obesity and type 2 diabetes, neurodevelopmental disorders, disorders associated with learning and memory such as autism spectrum disorders, and a majority of human cancers(5). Holding a central role in cell biology and having many disease implications, it is important to understand its mechanisms and regulation through the study of its rate-limiting step: translation initiation.

Eukaryotic Translation Initiation

There are two mechanisms of translation initiation in eukaryotic cells: cap-dependent and cap-independent translation initiation. The work presented herein will be relevant to cap-dependent translation initiation.

Cap-Dependent Translation Initiation

Under normal conditions, cap-dependent translation is the predominant mechanism of translation initiation in cells. Cap-dependent translation is reliant on the modified guanine residue at the 5' end of mRNA called the cap structure. The cap is a 7-methylguanosine linked to the first transcribed nucleotide of mRNA through a 5'-5' triphosphate bridge, and is often denoted as m^7GpppN (where N is any nucleotide and m is a methyl group)(6). Cap-dependent translation is mediated by the eukaryotic initiation factor (eIF) 4F complex which assembles on the 5' cap of mRNA and consists of the cap-binding protein eIF4E, the DEAD-box RNA helicase eIF4A, and the large scaffolding protein eIF4G. The details of the eIF4F complex are expanded on below. The RNA chaperones, eIF4B and eIF4H, interact with and stimulate eIF4A activity and facilitates ribosome recruitment(7). After eIF4F assembles on the 5' end of mRNA, the 43S pre-initiation complex (PIC) can be recruited. The 43S PIC is formed through the binding of eIF3, eIF1, eIF1A, eIF2•GTP •Met-tRNA$_i^{Met}$ and eIF5 to the small 40S ribosomal subunit(7). Interactions between eIF3 and eIF4G recruits the 40S ribosomal subunit to the mRNA, at which point the 43S PIC scans along the 5' untranslated region (UTR) of the mRNA until a start codon is recognized. At this point the initiation factors are evicted from the complex and eIF5B hydrolyzes a molecule of GTP in the recruitment of the large 60S ribosomal subunit to the small 40S subunit, forming the 80S complex, and elongation can begin(7). The poly(A)-binding protein (PABP), though not directly involved in translation initiation, interacts with eIF4G and is thought to circularize the mRNA, facilitating ribosome recycling and re-initiation(3,8). The process of cap-dependent translation is illustrated in Figure 1(9).

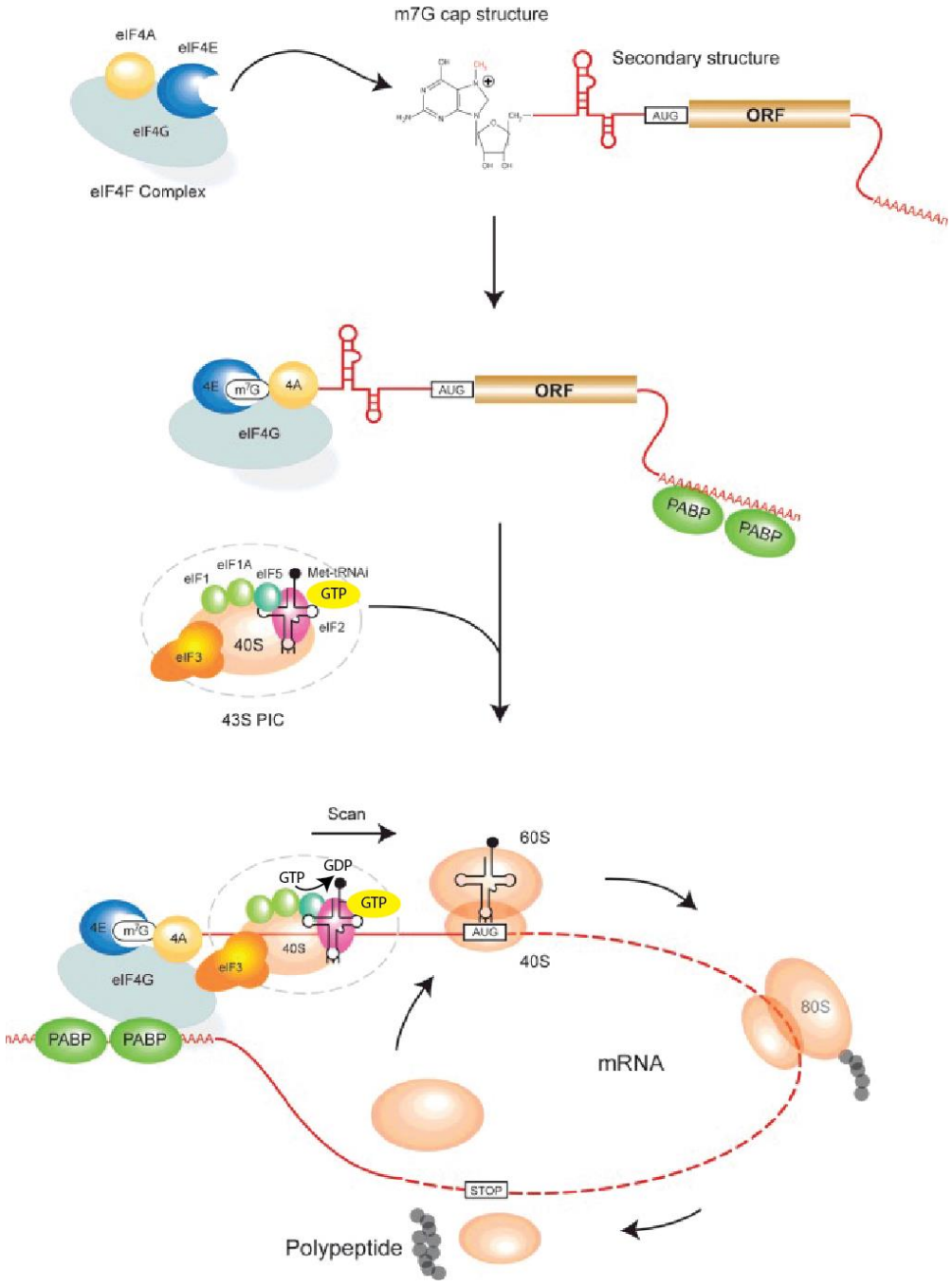

Figure 1. Cap-dependent translation initiation. The eIF4F complex assembles on the 5' cap structure of mRNA and facilitates the recruitment of the 43S PIC, which scans along the 5' UTR until the start codon is recognized. Upon start codon recognition, translation factors are evicted and the large 60S subunit of the ribosome is recruited to form the 80S translation competent ribosome and begin the elongation step. Figure modified from *Siddiqui and Sonenberg 2015(9)*.

Cap-Independent Translation Initiation

The best characterized mechanism of cap-independent translation initiation in eukaryotic cells are internal ribosome entry site (IRES) mediated translation initiation(10). The translation of mRNAs regulated by this non-canonical mechanisms is either cell-type specific or translation occurs during conditions of cellular stress, such as viral infection(11).

IRESes are highly structured elements in the mRNA which recruit the 40s subunit of the ribosome, eliminating the need for the 5' cap structure for translation initiation(12). IRES-mediated translation initiation may or may not use canonical eIFs and IRES-transacting factors (ITAFs), but rather is dependent on features of the mRNA for ribosomal recruitment (12). Mechanisms of 40S ribosomal subunit recruitment include formation of secondary and tertiary structures, interaction with ITAFs and Watson-Crick base pairing with the 18S ribosomal RNA (rRNA)(13). IRES elements are commonly used by viruses to subvert the host and promote the translation of viral transcripts while cap-dependent translation is compromised during cellular stress, and are best described in this context(14). The IRES was first described in RNA of poliovirus(10), and has since been described across a wide variety of viral transcripts. While most commonly described in the context of viral infection, IRESes have also been found to be present in cellular mRNAs(15). It has been reported that nearly 10% of cellular transcripts contain IRES elements(13). In the mammalian context, IRES-mediated translation is involved in the translation of specific mRNAs under conditions such as mitosis (ex.: vimentin, *CYR61*, *hnRNPA/B*), apoptosis (ex.: cyclin T1, Notch 2, *HeS1*) and hypoxia (ex.: *PDGF*, *VEGF*, *MMP13*), where cap-dependent translation capacities are reduced(16-18). Furthermore, under conditions of stress and apoptosis a subset of IRES-mediated mRNAs associated with proliferation, differentiation and regulation of apoptosis are selectively expressed, promoting survival and adaptation to these conditions(19).

The eIF4F Complex

The eIF4F complex functions to recruit ribosomes to mRNAs. It consists of three subunits: the DEAD-box RNA helicase eIF4A, the cap-binding protein eIF4E and the large scaffolding protein eIF4G.

eIF4A

eIF4A is the founding member of the DEAD-box helicase family and functions to unwind secondary structure in the mRNA in an ATP-dependent manner(3). There are two eIF4A paralogs in mammals which share 90% identity at the amino acid level, namely eIF4A1 and eIF4A2(3). *In vitro* these paralogs demonstrate similar activity and can participate interchangeably in the eIF4F complex(20), however there are significant differences in their activities *in vivo*(3). eIF4A1 is the predominantly expressed paralog under normal conditions and is an essential gene, while eIF4A2 is not an essential gene(21,22). *Eif4a2*, however, is essential for spermatogenesis in mice(22). eIF4A2 cannot compensate for loss of eIF4A1, although its expression is transcriptionally induced by the loss of eIF4A1(23). eIF4A is the most abundant translation factor in the cell at ~2.4 copies per ribosome, suggesting alternative roles for this protein outside the context of translation initiation(24).

Structurally, DEAD-box helicases have two recombinase A (RecA) domains connected by a flexible linker, forming a dumbbell shaped protein (Fig. 2A and B)(7,25). In the cleft between the two RecA domains lie the functionally relevant ATP and RNA-binding sites (Fig. 2B)(7,25). The unwinding of secondary structures occurs through repeated transitioning of opening and closing of the protein's conformation, which is coupled to RNA binding and subsequent ATP hydrolysis(3). The binding of eIF4E to eIF4G strongly stimulates eIF4A's helicase activity, independent of cap recognition and binding, promoting restructuring of the mRNA(26). eIF4B and eIF4H, the RNA chaperones, interact with and stimulate eIF4A activity, facilitating the recruitment of the ribosome(7).

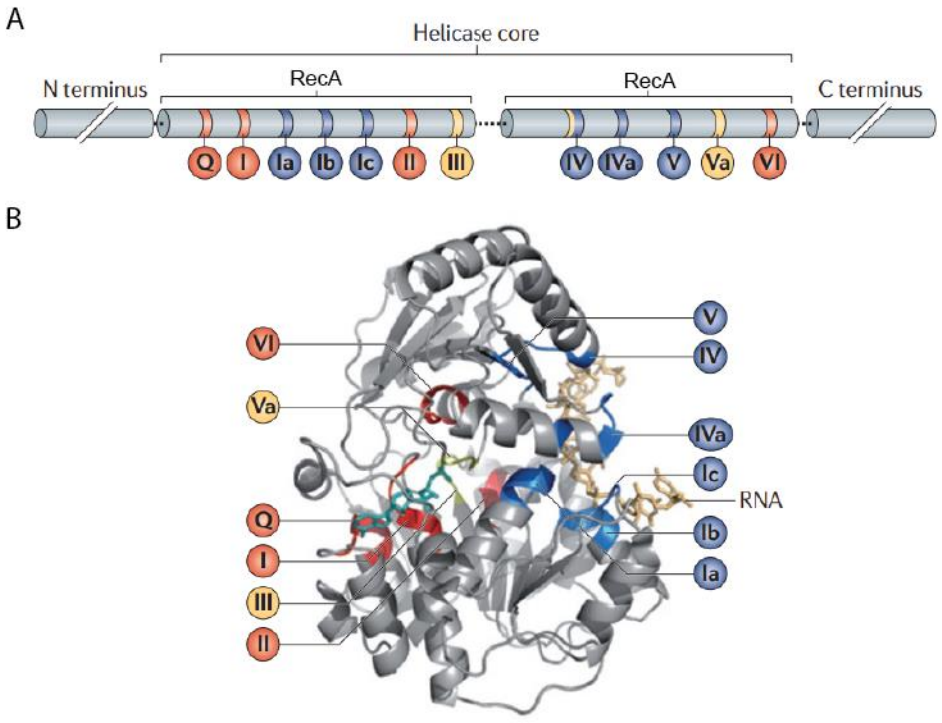

Figure 2. Structural features of eIF4A. The helicase core is composed of 2 RecA-like domains which house several conserved motifs associated with their characteristic function: ATP-binding and hydrolysis (red), RNA-binding (blue) and coordination between ATP- and RNA-binding sites (yellow) (A). These functional motifs arrange 3-dimensionally to form the catalytic cleft (B). Figure modified from *Linder and Jankowsky 2011(25)*.

eIF4H and eIF4B interact with eIF4A1 in a mutually exclusive manner as they share a common binding site for eIF4A1(27). Both these factors play important roles in the stimulation of eIF4A1 activity, although the effects on the stimulation of this activity in eIF4E-dependent ribosome recruitment remains unclear(3). In one model, binding of eIF4H or eIF4B to eIF4A1 stimulates ATP hydrolysis and subsequent promotion of the remodelling of the 5' UTR through eIF4A1's most commonly described function as an RNA helicase (Fig. 3)(28). This is consistent with observations that eIF4B, eIF4H and eIF4G enhance resolution of secondary structure of mRNA by eIF4A1 in an ATP-dependent manner, although eIF4H was less efficient at stimulating the unwinding activity(29). In the second model, ATP hydrolysis is stimulated by eIF4B or eIF4H and this facilitates clamping of eIF4A1 to mRNA (Fig. 3)(3). This mechanistic possibility is supported by observations that eIF4H enhances the clamping of eIF4A1 to RNA in the presence of silvestrol, a member of the rocaglate class of eIF4A inhibitors, in an RNA pull-down assay(30).

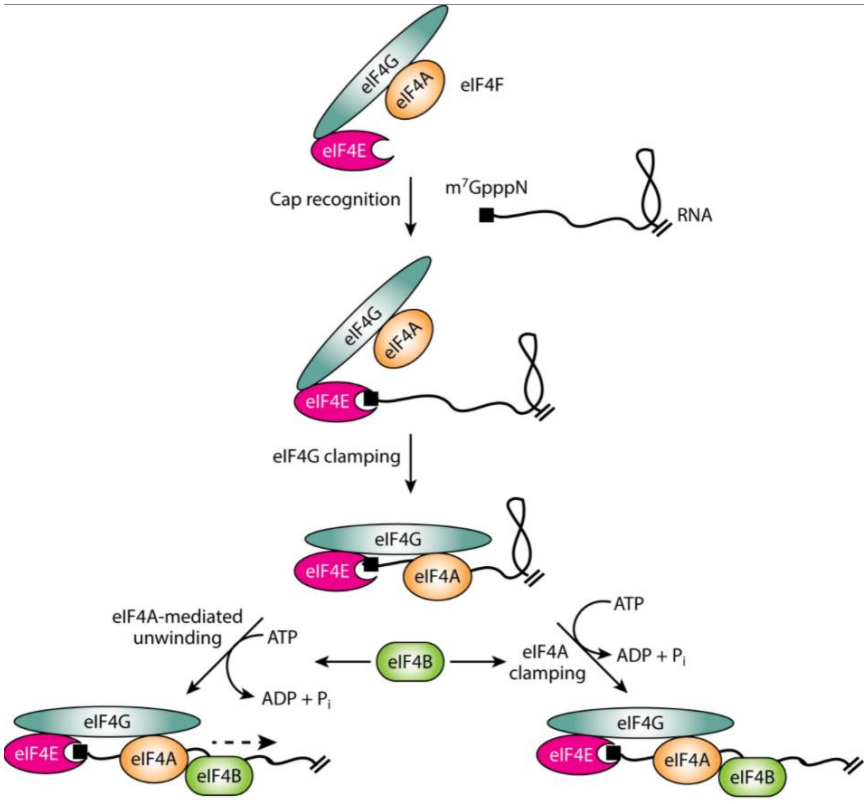

Figure 3. Alternative roles of eIF4A in eIF4E-dependent ribosome recruitment. Stimulation of eIF4A by eIF4B and/or eIF4H is thought to have two potential outcomes. In one model, stimulation of eIF4A induces the commonly described ATP-dependent RNA helicase activity of eIF4A (bottom left). Another model suggests an ATP driven clamping of eIF4A to the mRNA (bottom right). Figure obtained from *Pelletier and Sonenberg 2019(3)*.

eIF4G

The eIF4G proteins serve as large scaffolding proteins which hosts many of the factors associated with translation initiation. There are three eIF4G family members in mammals: eIF4G1 (eIF4GI), eIF4G2 (DAP5/p97/NAT1) and eIF4G3 (eIF4GII)(3). eIF4GI and eIF4GII share 46% identity in humans and have binding sites for the poly(A)-binding protein (PABP), eIF4E, eIF4A, eIF3 and MAP kinase-interacting kinase (MNK) (Fig. 4)(3,31). Both proteins can participate in the eIF4F complex and recruit ribosomes *in vitro*(20). *Eif4g1* is an essential gene, while *Eif4g3* is non-essential but was identified to play a critical role in spermatogenesis in the mouse(22). The N-terminal domain of eIF4GI and eIF4GII is the site of the PABP and eIF4E binding sites, and has been suggested to circularize the mRNA through interaction with both its 5’ cap and 3’ poly(A)

tail(32,33). However, this idea has been disputed, as single-molecule-resolution *in situ* hybridization (smFISH) experiments monitoring the 5' and 3' ends of translating mRNA shows that the two ends rarely colocalize which contradicts the mRNA circularization model(34,35). The middle domain of human eIF4G contains the first of three HEAT domains which bind eIF4A, and the C-terminal domain contains the other two HEAT domains(3). HEAT motifs are tandem repeats approximately 50 amino acids in length commonly involved in protein-protein interactions(36), and are present in multiple initiation factors(37). The first HEAT domain stimulates eIF4A's ATP hydrolysis and RNA binding activity(38). Binding of multiple HEAT domains to eIF4A is thought to keep eIF4A associated with eIF4G during its conformational changes associated with ATP hydrolysis and RNA unwinding(39). There are two RNA-binding domains (RBDs) in eIF4G, one N-terminal to the first HEAT domain and the second overlapping with it(40). The RBDs significantly enhance the interaction between the cap and eIF4E(41). MNK1 binds to the C-terminal domain of eIF4G through a HEAT domain. This binding promotes the phosphorylation of S209 of eIF4E by MNK1, reducing its affinity for the cap(42-44).

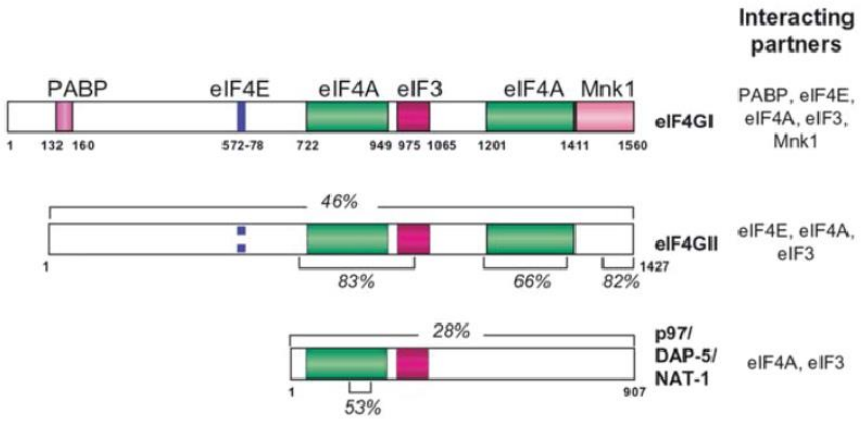

Figure 4. Structural features of eIF4G. eIF4GI contains binding domains for PABP (pink), eIF4E (blue), eIF4A (green), eIF3 (fuchsia) and Mnk1 (light pink). Amino acid identity of indicated regions in eIF4GII and p97/DAP-5/NAT-1 are shown as percent identity relative to eIF4GI. p97/DAP-5/NAT-1 lacks the N-terminal extension containing binding domains for PABP and eIF4E, and as such it cannot bind these proteins. Figure obtained from *Prévôt et al. 2003(31)*.

DAP5/p97/NAT1 lacks the N-terminal extension containing the PABP and eIF4E binding sites, rendering it functionally distinct from eIF4GI and eIF4GII as it does not support cap-dependent translation(31). eIF4G2 is an essential gene and is implicated in IRES-mediated

translation(3). Knock-down of DAP5/p97/NAT1 in embryonic stem cells impairs their ability to differentiate, and mouse embryos with this knock-down died during gastrulation, suggesting a critical function in embryogenesis(45).

eIF4E

There are three eIF4E family members in mammals: eIF4E-1 (eIF4E), eIF4E-2 (4EHP) and eIF4E-3 (eIF4E3)(46). They are ~25kDa in size with a disordered N-terminal domain followed by a conserved globular domain often described as a cupped hand(47). While eIF4E-1 is found in all eukaryotes, eIF4E-2 is restricted to metazoans and eIF4E-3 is restricted to chordates(46). eIF4E-1, hereinafter referred to as eIF4E, is an essential gene(22) and is the best characterized member of the eIF4E family. It recognizes the 5' m^7GpppN cap structure of mRNA through its ventral surface and interacts with both the mRNA and eIF4GI (Fig. 5A). The canonical eIF4E-binding motif (4EBM) of eIF4GI interacts with a conserved pocket of hydrophobic residues on the dorsal surface of eIF4E (Fig. 5B)(48,49). The binding of eIF4E to the cap structure is mediated by sandwiching the m^7G base of the cap between the indole side chains of tryptophan W56 and W102 (Fig. 5C)(3). The cap-binding is further stabilized through three Watson-Crick-like hydrogen bonds between a side-chain carboxylate of glutamine E103 and the N1 and N2 hydrogens of the N7-methylguanosine moiety, as well as interaction of E103 with W102 (Fig. 5C)(3,50). Cap-binding is further mediated by a number of other interactions between charged side chains or water and the phosphates (Fig. 5C)(3,50). The N7 methyl residue is very important for cap-recognition as it ensures the modified nucleotide remains in the *anti*-conformation, which is more accessible to recognition by eIF4E than the *syn*-conformation(3).

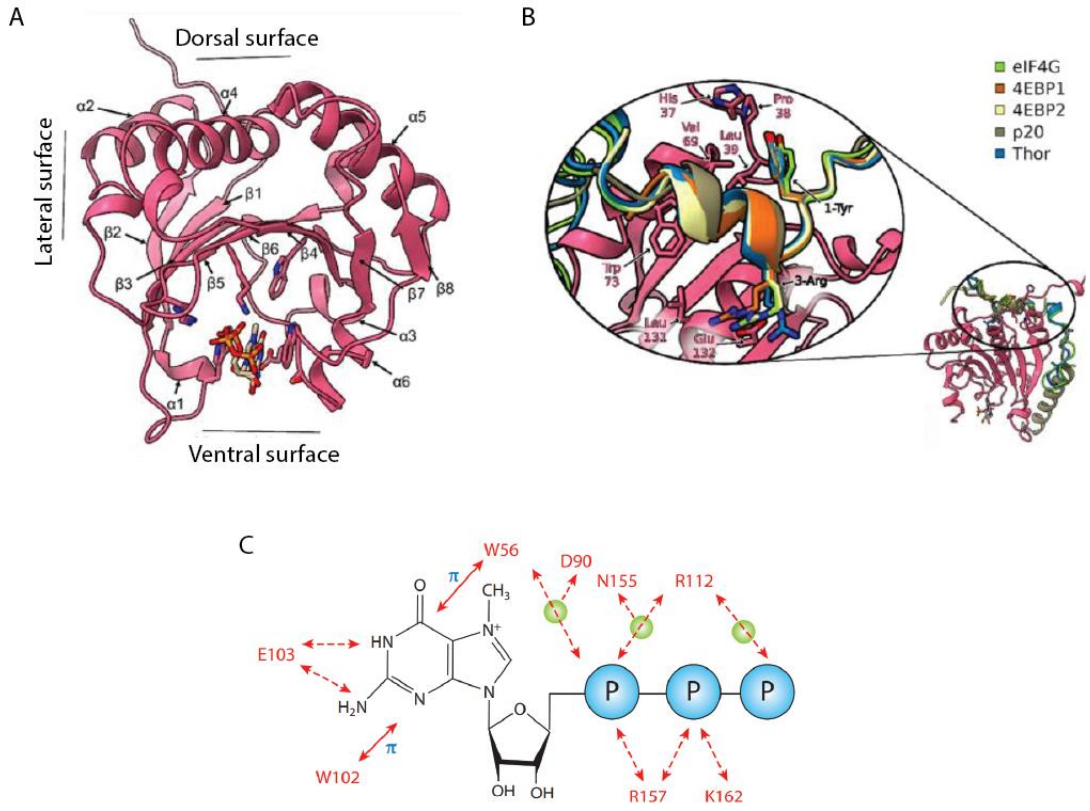

Figure 5. Structure of eIF4E and interactions between key eIF4E residues and the 5' m^7GpppN cap structure of mRNA. (A) The cap-binding pocket, shown in stick structure, is located on the ventral surface of eIF4E. (B) The dorsal surface contains a conserved pocket of hydrophobic residues recognized by the canonical eIF4E-binding motif (4EBM). (C) The m^7G base of the cap structure is sandwiched between the aromatic indole side chains of W56 and W102. Further interactions are made via Watson-Crick-like hydrogen bonding of E103, and other interactions between phosphates or water and the phosphates. Figure modified from *Romagnoli et al. 2021(48)* (A and B) and obtained from *Pelletier and Sonenberg 2019(3)* (C).

eIF4E is the rate-limiting factor in eIF4F assembly, and in turn levels of eIF4E determine rates of translation initiation. It is estimated that there are ~0.1 molecules of eIF4E per ribosome in exponentially growing cells(24). Cells are especially sensitive to changes in eIF4E levels, as even a 2.5-fold increase in eIF4E levels is sufficient to drive tumorigenesis as first described in the transformation of mouse embryonic fibroblasts through eIF4E overexpression(51,52). In fact, eIF4E is qualified as a proto-oncoprotein(53), and as such its levels are tightly regulated. Details of this regulation and the role of eIF4E in disease will be further detailed below.

4EHP, or eIF4E-2, shares only 28% identity to human eIF4E(46). Unlike eIF4E, 4EHP cannot interact with eIF4GI(47). 4EHP is 5-10 times less abundant than eIF4E across a variety of

mammalian cell lines and is ubiquitously expressed (54,55). The affinity of 4EHP to cap analogs m^7GpppG and m^7GTP is 30 and 100-fold weaker, respectively, than eIF4E(56). This discrepancy in affinity is due to a two-amino acid substitution in the cap-binding pocket(56). While 4EHP cannot compete with eIF4E to bind the cap structure of most mRNAs, it has been predominantly documented as a translational repressor(56,57). 4EHP has been documented to interact with RNA binding proteins to mediate its translational repression, and recently has been shown to be an integral component in miRNA-mediated translational repression(57).

eIF4E3 is the least studied eIF4E family member. It shares 29% identity with eIF4E1, and its expression is limited to the spleen, muscle, and lung, contrasting the ubiquitous expression of eIF4E and 4EHP(3,46). eIF4E3 can bind to the cap structure with similar affinity to 4EHP, but binds with less specificity than eIF4E(46,58). Its cap-binding mechanism is unique in that it does not bind the guanine base of the cap with an aromatic sandwich and instead makes its second contact with a cysteine residue(58). A variety of other electrostatic and Van der Waals contacts further stabilize the interaction(58). The contacts between eIF4E3 and the cap are far more extensive than eIF4E and 4EHP(58). Similar to eIF4E, eIF4E3 is able to bind to a fragment of eIF4GI *in vitro*(46). eIF4E3 is thought to act as a tumor suppressor protein due to its competition with eIF4E, serving to downregulate translation initiation(58). While eIF4E3's activity is physiologically relevant, details of its functional role remain unclear and require further investigation.

Cellular Context of eIF4E

eIF4E interacts with mRNA and facilitates the recruitment of the 40S ribosomal subunit. As the rate-limiting factor in translation initiation, it has many implications in the regulation of this process and many cancers are associated with dysregulation of this initiation factor.

Regulation of eIF4E availability

As the rate-limiting initiation factor in eIF4F complex assembly, the availability of eIF4E is tightly regulated. Activity and availability of eIF4E is controlled by amplification of the gene encoding eIF4E, transcriptional activation, sequestration of eIF4E by the eIF4E-binding proteins (4EBPs) and post-translational modification of eIF4E, namely phosphorylation(59). Numerous stimuli have been shown to induce eIF4E expression. eIF4E mRNA levels have been observed to increase several-fold in fibroblasts treated with serum or growth factors(60). Additionally, a rapid increase in eIF4E mRNA levels has been detected during activation of quiescent T cells, a response to the demand imposed by a surge in protein synthesis rates(61). Overexpression of eIF4E is mediated by the MYC transcriptional activation program, and as such increased eIF4E levels have been documented in head and neck squamous cell carcinomas(62).

The sequestration of eIF4E by the 4EBPs is mediated by mechanistic/mammalian target of rapamycin (mTOR). mTOR is a highly conserved serine/threonine kinase which forms in two complexes with distinct function, namely mTORC1 and mTORC2, and is a master-regulator of growth at the cellular, organ and organismal level(63). mTOR controls many cellular processes such as protein synthesis, cell growth and proliferation, lipid metabolism, cytoskeletal organization, mitochondrial function, and autophagy(9,64). mTORC2 contains the subunit Rictor, among others, and exerts downstream effects on ion transport, apoptosis, glucose metabolism, cell migration and cytoskeletal rearrangement(65). mTORC1 contains the subunit Raptor which functions as an adaptor allowing it to target its substrate 4EBPs and S6 kinases, among others(64). It integrates a multitude of intracellular and extracellular cues such as mitogen and growth factor signaling, energy levels, genotoxic stress, and oxygen availability(63). It is activated in the PI3K/Akt/mTOR signalling cascade through ordered serine/threonine phosphorylation and GTPase events(66). mTORC1 plays a major role in translational control, and it mainly exerts this function through controlling activation of the 4EBPs. Activation of 4EPBs is mediated via

phosphorylation, which in turns influences the affinity of the 4EBPs for eIF4E(67). In the hyperphosphorylated form, such as under conditions of mTORC1 activation, 4EBPs have decreased affinity for eIF4E, freeing it for eIF4F complex formation and promoting translation initiation(67,68).

Lastly, eIF4E activity is modulated via phosphorylation of a single residue, serine S209, by MNKs. Phosphorylation of eIF4E is correlated with translation rates and growth status of cells, and plays a role in cancer development and progression(42,69). MNKs act as downstream effectors in the MEK-ERK and p38 MAPK pathways, and as such the phosphorylation of eIF4E is determined by stimuli such as mitogenic signals and stress (59). Phosphorylation of eIF4E occurs through the docking of MNKs to eIF4G, which is facilitated by the eIF3e subunit of eIF3(70). This phosphorylation plays important roles in cell proliferation, transformation, immune response, and viral infection(70). The role of eIF4E phosphorylation in cancer is of particular interest, as expression of a non-phosphorylatable eIF4E (S209A) in a mouse prostate cancer model was sufficient to delay tumor onset(71). Phosphorylation of eIF4E does not modulate global translation rates but rather stimulates the translation of a subset of mRNAs associated with survival and invasion, such as myeloid cell leukemia 1 (*MCL1*) and matrix metalloproteinase 3 (*MMP3*)(71,72).

4E-sensitive mRNAs

Interestingly, not all mRNAs are equally affected by changes in eIF4E levels. A subset of mRNAs called eIF4E-sensitive mRNAs are disproportionately affected by fluxes in eIF4E levels(73). Under normal conditions eIF4F complex formation is rate limiting for translation initiation, as 4EBPs sequester eIF4E from the eIF4F complex(73). However, under conditions of increased mTOR activation eIF4E is released from the 4EBPs and the eIF4F complex forms more freely, changing the landscape of the translatome through promoting the translation of eIF4E-sensitive mRNAs. This discrepancy in dependence on eIF4E for efficient translation is due to the so-called “translatability” of the mRNA, which is largely dependent on features within the 5’ UTR(73). This variability in translatability is quite large; the translation efficiency of mRNAs can vary over a 100-fold range in metazoans(74). eIF4E-sensitive mRNAs tend to have 5’UTRs that are G+C rich, highly structured and lengthy(73). Additionally, mRNAs engineered to have higher degree of secondary structure in the 5’ UTR were selectively upregulated in cells overexpressing eIF4E(75). These are also termed “weak” mRNAs due to their poorer translatability, as such

features of the 5'UTR lead to a greater dependency on the eIF4F complex for unwinding, scanning, start codon recognition and ribosome loading(73). The eIF4E-sensitive mRNAs tend to encode growth and survival factors such as c-myc, vascular endothelial growth factor (*VEGF*), cyclins, ornithine decarboxylase (*ODC*) and survivin (Fig. 6)(60,76,77). Most cellular mRNAs, however, do not have 5' UTRs with such characteristics and are less dependent on the eIF4F complex for efficient translation. These are "strong" mRNAs and encode most cellular proteins and housekeeping genes, such as β-actin and glyceraldehyde-3-phosphate dehydrogenase (*GAPDH*) (Fig. 6)(73).

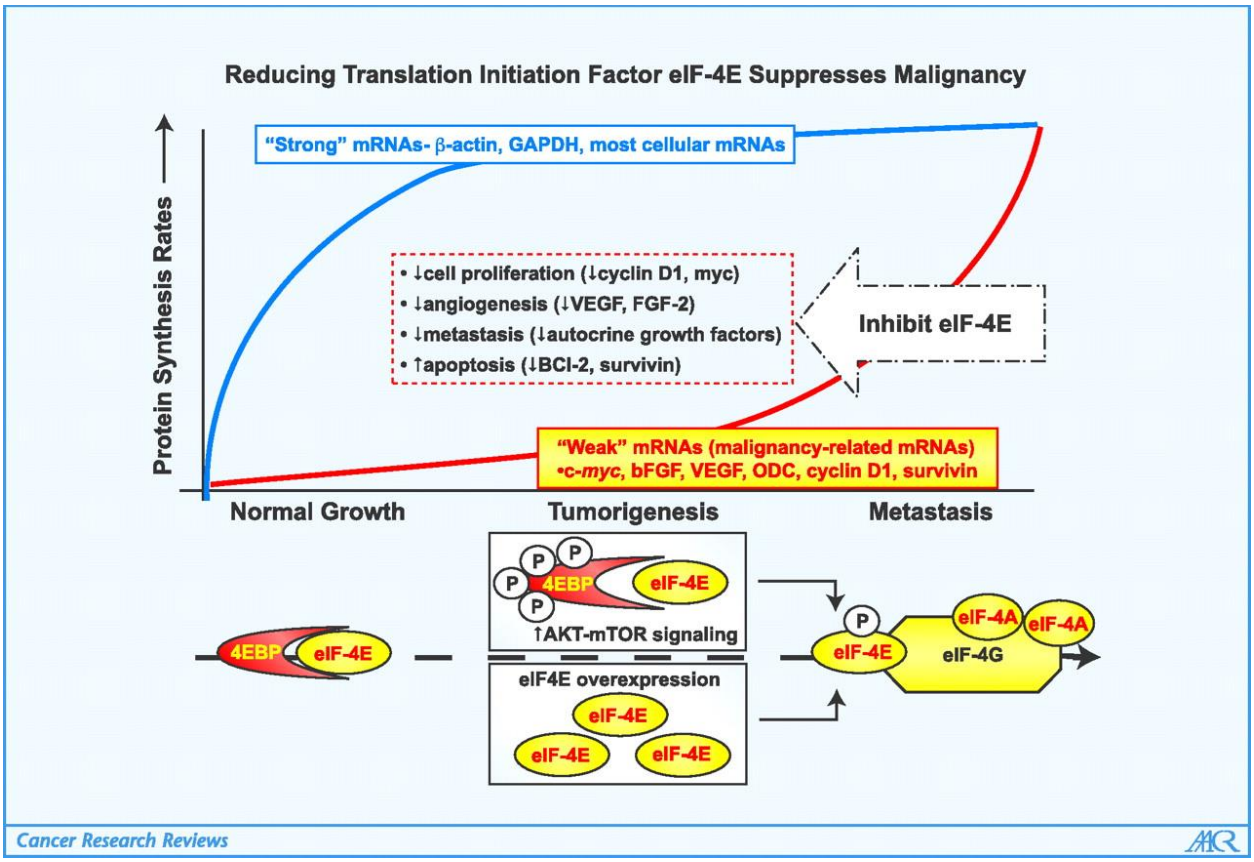

Figure 6. eIF4E-sensitive mRNAs. Features of the 5' UTR determine the sensitivity of an mRNA to fluxes in eIF4E levels. "Weak" mRNAs are most sensitive to eIF4E availability and tend to encode malignancy-related genes such as c-Myc, VEGF, cyclin D1 and survivin. eIF4E availability is largely regulated through sequestration by 4EBPs. Figure obtained from *Graff et al. 2008(73).*

Role of eIF4E in cancer

Perhaps not surprisingly, dysregulation of eIF4E levels is heavily associated with poor outcomes in a number of cancers. As described previously, increased availability of eIF4E selectively upregulates a number of malignancy-associated mRNAs encoding proto-oncoproteins as well as growth, pro-angiogenic and survival factors(73). In addition to translational effects, overexpression of eIF4E in mouse embryonic fibroblasts was shown to increase nucleocytoplasmic transport of the potent growth regulatory protein cyclin D1(52). Increased expression of eIF4E was found to be associated with transformation in fibroblasts(51). Also noted in primary rodent fibroblasts was a cooperation of eIF4E with v-*myc* and E1A, both immortalizing oncogenes, to enhance transformation(78). In a lymphoma-prone mouse model, named the *Eμ-Myc* model, hemizygosity at the *Eif4e* locus delayed tumor onset(22). Activation of eIF4E was also found to be a key event in lymphomagenesis *in vivo*, and functioned cooperatively with c-Myc(79). eIF4E was found to play a central role in tumor growth, invasion and metastasis in an *in vivo* model(80). In this model, CREF tumor cells transfected to ectopically express eIF4E were found to be capable of spontaneously metastasizing to the lung. The metastases were harvested and showed greater eIF4E expression than the original transfected parental cells, suggesting this expression is selected for in the metastatic process(80). eIF4E overexpression is also involved in establishing autocrine stimulatory loops that foster *ras*-MAPK signaling(81), and suppress endoplasmic reticulum-mediated apoptosis(82). In addition to promoting tumorigenesis, disease progression, angiogenesis and metastasis, eIF4E overexpression can also impart drug(83) and radioresistance(4). eIF4E is found to be overexpressed in a variety of human cancers including breast, head and neck, colorectal, bladder, prostate adenocarcinoma, lung, cervical and lymphomas(4). In all, increased eIF4E availability has been extensively linked to tumorigenesis and cancer progression.

eIF4E-Binding Proteins

The 4EBPs are a family of translational repressors that consists of three homologs in mammals, namely 4EBP1, 4EBP2 and 4EBP3, which share ~60% identity(84). They tightly regulate the availability of eIF4E by competing with the scaffolding protein eIF4G for binding of eIF4E(85). These proteins are ubiquitously expressed across all tissue but expression levels vary: 4EBP1 is highly expressed in skeletal muscle, pancreas and adipose tissue, 4EBP2 is predominantly expressed in the brain and lymphocytes, and 4EBP3 is expressed at low levels across all tissues(84,86,87) The 4EBPs, specifically 4EBP1 and 4EBP2, were first identified to function as inhibitors of translation in 1994 through interference with eIF4F complex formation(85). The best characterized 4EBP is 4EBP1 and is the homolog that will be focused on henceforth.

Binding mechanism of the 4EBPs

While eIF4G and 4EBP1 both bind eIF4E with a similar affinity(88), their binding mechanisms differ, relevant to their physiological function. Common to both eIF4G and 4EBP1 is the canonical eIF4E binding motif (4EBM) which has the sequence YXXXXLΦ, where Y denotes tyrosine, X is any amino acid, L denotes leucine and Φ is a hydrophobic residue(89,90). This motif binds to a conserved patch of hydrophobic residues on the dorsal side of eIF4E (Fig. 7A and B)(49). Present in 4EBP1, but not in eIF4G, is a non-canonical 4EBM, which is located downstream of the canonical 4EBM after a flexible linker of 15-30 residues called the elbow loop(91). The non-canonical 4EBM binds the lateral surface of eIF4E (Fig. 7A)(91,92). Unlike the canonical 4EBM, the non-canonical 4EBMs do not share sequence similarity and are not conserved in 4EBP orthologs(88). However, it has been shown through structural resolution of 4EBP orthologs bound to eIF4E that the non-canonical motifs all bind the lateral surface of eIF4E, despite not sharing sequence similarity(88,91,93). The non-canonical 4EBM significantly increases the affinity of the 4EBPs for eIF4E (94). In human 4EBP1 and 4EBP2, the non-canonical 4EBM was determined to increase the binding affinity for eIF4E by approximately three orders of magnitude(94,95). Its effects on affinity for eIF4E, along with structural advantages, makes the non-canonical 4EBM a requirement for 4EBPs to compete with eIF4G for eIF4E binding(88,95).

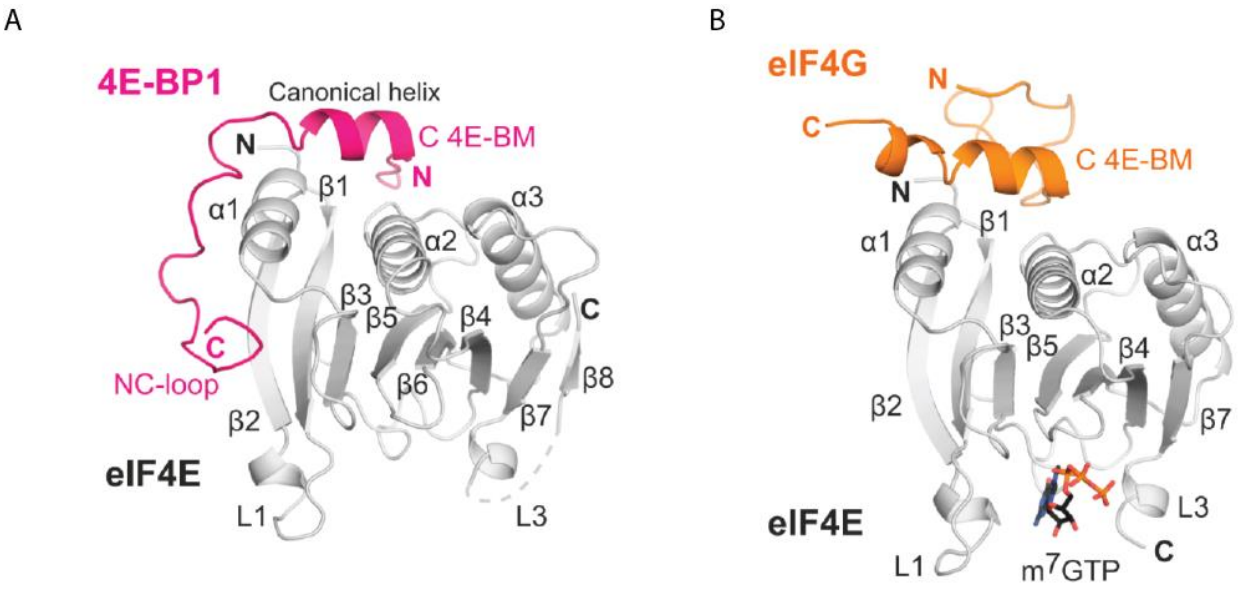

Figure 7. Structure of 4EBP1 and eIF4G bound to eIF4E. The canonical 4EBM (C 4E-BM) is found in both (A) 4EBP1 and (B) eIF4G and binds to the dorsal surface of eIF4E (shown in grey). (A) The 4EBPs have an additional non-canonical 4EBM (NC-loop) which binds the lateral surface of eIF4E. (B) eIF4G does not contain a non-canonical 4EBM. Figure adapted from *Peter et al. 2015 (91)*.

An important advancement in the understanding of the competition for eIF4E binding between eIF4G and the 4EBPs was made through the determination of high-resolution structures of eIF4E bound to both these proteins (Fig. 7)(91). In 4EBPs, the elbow loop and non-canonical 4EBM are sufficient for binding to eIF4E *in vitro* as determined through observed continued binding activity after abolishing the canonical 4EBM(88). Contrastingly, abolishing the canonical 4EBM in eIF4G completely inhibits its ability to bind eIF4E(91). This is evidence that 4EBPs bind eIF4E in a truly bipartite mechanism(88). These findings and structural determinations have led to the development of the current working model for how the 4EBPs compete with eIF4G for eIF4E binding. It is suggested that the 4EBPs bind eIF4E while eIF4E is within the eIF4F complex through docking to the lateral surface of eIF4E, where it is then primed to compete with eIF4G for binding the dorsal surface of eIF4E through the canonical 4EBM(91). Also involved in this competition are two phosphorylation sites, S65 and T70, present in the elbow loop. While these sites do not directly interface with eIF4E, it has been shown that phosphorylation at these sites in 4EBP orthologs impairs their ability to displace eIF4G from eIF4E, strongly implicating these phosphorylation sites in the competition mechanism(91).

4EBPs are known to be intrinsically disordered proteins(90). High-resolution X-ray crystallography has previously revealed that recognition of the conserved hydrophobic patch on the dorsal surface of eIF4E induces a disorder-to-order transition(90). Later studies revealed that recognition of the dorsal surface of eIF4E induces a partial folding of eIF4E, and that the disordered nature of the non-canonical 4EBM gives it the advantage of better "catching" the lateral surface of eIF4E(93). The 4EBPs have also been found to have a kinetic advantage for binding over eIF4G, giving them a competitive advantage due to the nature of the non-canonical 4EBM(88). Binding of the non-canonical 4EBM to eIF4E strengthens the interaction through a wrapping mechanism, and generally covers a much larger region as it is not confined to a classical single conformational state(93,96). The transition of 4EBPs from disordered to ordered structure has also been linked to the phosphorylation status of the protein(97). This has been shown in 4EBP2, where phosphorylation at residues T37 and T46 induces a partial folding, burying the canonical 4EBM into a four-stranded β-domain and blocking its accessibility to eIF4E(97). The weak nature of this partial fold reduces its affinity to eIF4E, but it can still undergo a disorder-to-order transition upon binding to eIF4E(97).

Phosphorylation of 4EBPs

The activity level of the 4EBPs, particularly 4EBP1 and 4EBP2, is determined through their phosphorylation state(68,98). In the hypophosphorylated state 4EBPs interact strongly with eIF4E, while the affinity for eIF4E is dramatically reduced upon phosphorylation(98). The activation of the PI3K/Akt/mTOR signaling pathway leads to the phosphorylation of 4EBPs by mTORC1 at multiple sites to cause their dissociation from eIF4E, freeing it to form as part of eIF4F assembly(99,100). Conversely, treatment of mouse embryonic fibroblasts with the mTORC1 inhibitor rapamycin blocks the phosphorylation of 4EBP1 and inhibits cap-dependent translation(100). 4EBP1 is one of several targets of mTORC1 directly involved in the negative regulation of translation. Ribosomal S6 kinases 1 and 2 (S6Ks) activation by mTORC1 leads to the phosphorylation of programmed cell death protein 4 (PDCD4), ribosomal protein S6 (rpS6), eIF4B, eIF4H and eukaryotic elongation factor 2 (eEF2)(66,99). Reducing mTORC1 activation through nutrient or growth factor deprivation leads to dephosphorylation of 4EBP1, increasing its binding to eIF4E and in turn decreasing rates of cap-dependent translation(69,101,102). Viral

infection, such as encephalomyocarditis virus (EMCV) infection, can also lead to dephosphorylation of 4EBP1 and shutoff of host protein synthesis(103).

Phosphorylation of the 4EBPs occurs in a stepwise manner and has been described in 4EBP1 and 4EBP2, as will be detailed here. The regulation of 4EBP3 has been less studied and remains unclear(104). The mechanism of this phenomenon has been most studied in 4EBP1, where seven phosphorylation sites have been identified: T37, T46, S65, T70, S83, S101 and S112(105-108). The first two phosphorylation sites, T37 and T46, are phosphorylated under baseline conditions and act as a "primer" for phosphorylation of subsequent sites (Fig. 8)(98). Treatment of HEK293T cells with serum only moderately increased the phosphorylation at these sites(98). The serum and rapamycin-responsive phosphorylation sites are S65 and T70, as first determined through two-dimensional isoelectric-focusing/SDS-PAGE(109). Phosphorylation of the first two sites, T37 and T46, is required for subsequent phosphorylation of T70 followed by S65 (Fig. 8)(109). Phosphorylation of S65 and T70 alone is insufficient to disrupt eIF4E binding activity, indicating that the multiple phosphorylation events are required for release of eIF4E(109). This is consistent with the observation that S65 and T70 phosphorylation is involved in the competition mechanism for displacement of eIF4E from eIF4G by 4EBPs rather than direct eIF4E binding(91). The first four phosphorylation sites are conserved across 4EBP1 and 4EBP2 and behave in the same manner in both proteins(98,109,110). Two phosphorylation sites, S101 and S112, are conserved in 4EBP1 in mammals that are not found in 4EBP2 or 4EBP3(106,108). Uniquely, S112 can directly affect eIF4E binding activity independently of phosphorylation at other sites(108). Also in 4EBP1, phosphorylation at S101 is required for efficient phosphorylation of S65 (Fig. 8)(108). The last phosphorylation site in 4EBP1, S83, is conserved across all the 4EBPs although it does not seem to have a relevant role in eIF4E binding capabilities or translational control(53).

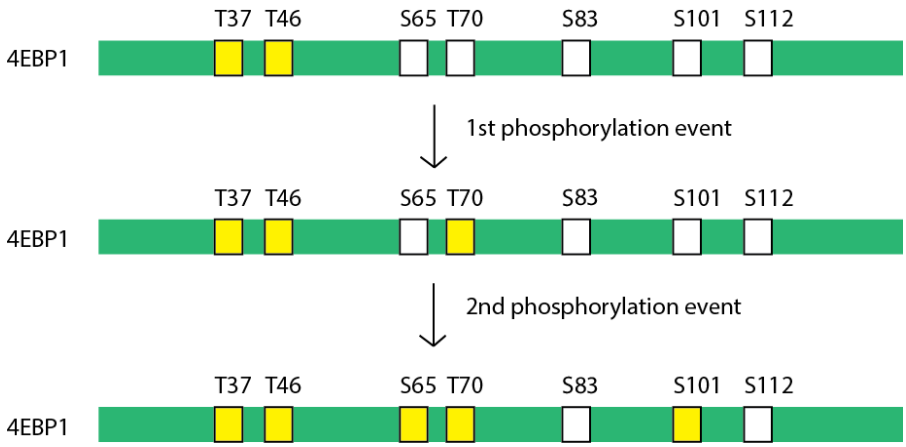

Figure 8. Conserved phosphorylation sites and sequential phosphorylation of human 4EBP1. Under baseline conditions, T37 and T46 are phosphorylated as shown by yellow boxes (top). T70 is the next residue to be phosphorylated by mTORC1 (middle), followed by S65 (bottom). In 4EBP1, phosphorylation at S101 is required for efficient phosphorylation of S65 (bottom). The details of phosphorylation events at S83 and S112 are not known.

Roles of 4EBPs in disease

All three members of the 4EBP family have been associated with disease states. The best characterized role of 4EBP in disease is that of 4EBP1 in cancer. The role of 4EBP1 in cancer is two-sided and context-dependent: on one hand it plays a protective, tumor-suppressor role through the sequestration of eIF4E and subsequent limitation of protein synthesis under normal cellular conditions(111,112). On the other hand, it can have a pro-tumorigenic role in the context of cancers through the selective upregulation of 4E-sensitive mRNAs as previously described(4). A number of studies have identified 4EBP1 hyperphosphorylation across many cancer types (Table 1). Overexpression of hyperphosphorylated 4EBP1 is positively correlated with different adverse outcome variables in these cancers, including poor prognosis, relapse, increased tumor size, poor differentiation, and metastasis(113). In its hyperphosphorylated form, 4EBP1 releases eIF4E and allows the tumor cell to adapt to its microenvironment through remodelling of the translational landscape and upregulation of the expression of key transcripts(113). It has been reported that hyperphosphorylated 4EBP1 upregulates translation of a number of transcripts involved in cell cycle progression, namely cyclin B1, D1, E and Cyclin dependent kinases 1 and 2, while their mRNA levels remained unchanged(114). Inhibiting mTORC1, and downstream phosphorylation

of 4EBP1 with rapamycin, blocked this upregulation(114). 4EBP1, as well as S6K1, has been described as a regulator of cell size as a major downstream effector of mTOR(115,116). 4EBP1 phosphorylation and activation of S6K1 also accelerates entry into S-phase, driving cell-cycle progression(115). In primary fibroblasts expressing p53, a tumor suppressor gene that promotes apoptosis, cell cycle arrest, and senescence(117), knock-down of 4EBP1 and 4EBP2 leads to resistance of oncogene-driven transformation and premature senescence(118). In advanced breast carcinomas, overexpression of 4EBP1 led to a hypoxia-induced switch from cap-dependent to cap-independent translation which promoted translation of the pro-angiogenic factors HIF-1α and VEGF(119). Knock-down of 4EBP1 with shRNA in glioblastoma led to an increase in sensitivity to hypoxia-induced death *in vitro* and radiation treatment *in vivo* (120). In breast cancer, elevated 4EBP1 mRNA levels have been determined to be an independent prognostic factor for poor outcomes(121,122). With defined mechanisms and its frequent deregulations across many cancer types, 4EBP1 has been called a master regulator of translation in the tumorigenic context(113).

Table 1: Alterations of 4EBP1 and eIF4E have been reported across many human cancers.

Malignancy	***4EBP1 alteration***	***eIF4E alteration***
Acute lymphatic leukemia (Nemes et al. 2013)(123)	Elevated p-4EBP1	Not reported
Acute myeloid leukemia (Chen et al. 2010)(124)	Elevated p-4EBP1	Elevated eIF4E
Bladder, urothelial carcinoma (Schultz et al. 2010)(125)	Elevated 4EBP1	Not reported
Breast cancer (Rojo et al. 2007) (126)	Elevated p-4EBP1	Not reported
Colorectal carcinoma (Zhang et al. 2009)(127)	Elevated p-4EBP1	Not reported
Endometrial cancer (Rice et al. 2006)(128)	Elevated p-4EBP1	Not reported
Esophageal cancer (Salehi and Mashayekhi 2006)(129)	Elevated 4EBP1	Elevated eIF4E
Gastric cancer (Jiao et al. 2013)(130)	Elevated 4EBP1 and p-4EBP1	Not reported
Gliomas, pediatric (Mueller et al. 2012)(131)	Elevated p-4EBP1	Not reported
Head and neck squamous cell carcinoma (Clark et al. 2010, De Benedetti and Graff 2004)(4,132)	Elevated p-4EBP1	Elevated eIF4E
Lung cancer, non-small cell (Lee et al. 2015)(133)	Elevated p-4EBP1	Not reported
Lymphoma, non-Hodgkin's (De Benedetti and Graff 2004)(4)	Not reported	Elevated eIF4E
Neuroblastoma (Iżycka-Świeszewska et al. 2010)(134)	Elevated p-4EBP1	Not reported
Ovarian carcinoma (Castellvi et al. 2006) (135)	Elevated p-4EBP1	Not reported
Prostate cancer (Graff et al. 2009)(136)	Elevated p-4EBP1	Not reported

(Adapted from Musa et al. 2015)

4EBP2 is the 4EBP family member predominantly expressed in the brain and has long been recognized to play an important role in learning and memory(137). These effects were first described in 4EBP2 knock-out mice, who were found to have impaired spatial learning and memory and failed to develop fear-associative memory(137). In recent years, two studies have linked loss of 4EBP2 to the development of autism spectrum disorder (ASD) associated behaviours

in mice(138,139). ASD is thought to be caused by hyperconnectivity of neuronal circuits through increased synaptic protein synthesis(139). Loss of 4EBP2 or overexpression of eIF4E in mice led to an increased translation of neuroligin mRNAs which are causative of ASD(139). 4EBP2 knock-out mice displayed autistic phenotypes commonly reported in humans, such as impaired social and repetitive behaviours(139). Another study where 4EBP2 deletion was systematically induced in a cell-type-specific manner mapped the deletion of 4EBP2 in inhibitory interneurons to be responsible for autistic-like behaviours(138). Both these findings are consistent with the previous observation that dysregulation of cap-dependent translation is a cause of ASD(140). Deletion of 4EBP2 in Purkinje cells, which are cerebellar cortex-specific neurons, in mice leads to deficits in motor learning and spatial memory(141). ASD-like behaviour is not observed in these mice, as they did not display deficits in social or repetitive behaviour(141). This suggests distinct roles and mechanisms of 4EBP2 in different cognitive processes across cell types and regions of the brain, and these roles remain an active area of research.

While 4EBP1 and 4EBP2 are regulated through their phosphorylation status, evidence suggests that 4EBP3 is primarily regulated at the level of transcription(142). 4EBP3 is poorly phosphorylated, further distinguishing its mechanism of regulation from that of the other 4EBP family members(84). In a chemically-induced liver cancer model given prolonged treatment with mTOR inhibitors, 4EBP3 was found to be transcriptionally induced, which was further validated *in vitro*(143). The induction of 4EBP3 was shown to occur through the transcription factor TFE3, which is activated by mTORC1 inhibition(144,145). In this model, 4EBP3 was found to suppress translation of eIF4E-sensitive mRNAs and exert anti-proliferative effects(143). This study suggests 4EBP3 to be important in maintaining translational repression during prolonged mTORC1 inhibition(143). It was also found that 4EBP3 mRNA levels were inversely correlated with activation of mTORC1 in breast cancer patients, further supporting the model of transcriptional induction(143). These studies show 4EBP3 to be a robust predictive biomarker of the therapeutic response to prolonged treatment with mTOR inhibitors(143).

Overview and Rationale for Thesis

In 2017, Sonenberg and colleagues published the results of a BioID assay(146) seeking to identify novel interacting partners of eIF4E and 4EHP (Fig. 9)(57). In this assay, a promiscuous biotin ligase is fused to the N- or C-terminus of eIF4E or 4EHP and stably expressed in cells. Biotinylated proteins were then isolated using a streptavidin-affinity purification and identified using mass spectrometry (146). A protein of unknown function, C8Orf88, was found to be a high-confidence target of eIF4E, but not 4EHP (Fig. 9)(57). PARP12 was also identified to interact with eIF4E and not 4EHP, however its interaction with the translation machinery has previously been described(147). Gene Ontology (GO) analysis, a computational tool combining experimental data and information on conserved sequences to inform on gene function, predicts C8Orf88 to be an eIF4E binding protein as well as a negative regulator of translation(148).

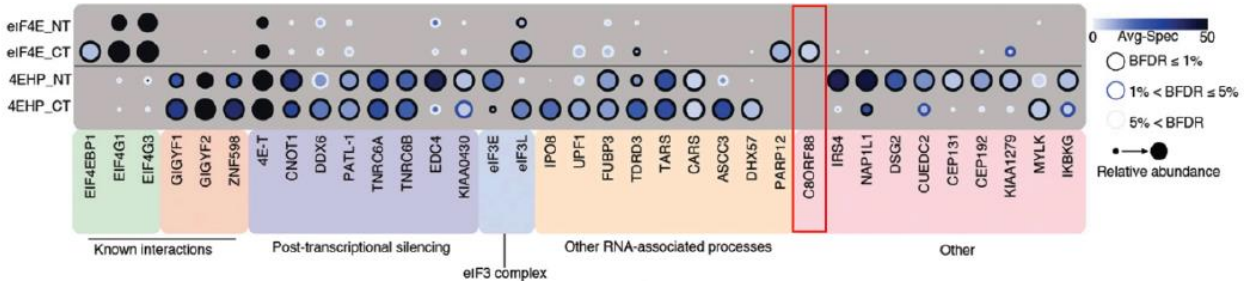

Figure 9. BioID assay results suggests an interaction between eIF4E and C8Orf88. A promiscuous biotin ligase was fused to both the N- and C-terminal domains of eIF4E and 4EHP and expressed in HEK293T cells. Biotinylated proteins were isolated by streptavidin-affinity purification and identified using mass spectrometry. The abundance, Bayesian false discovery rate (BFDR) and average spectral counts are displayed for all high-confidence targets identified above. C8Orf88 (red box) was found to be a high confidence interacting partner with eIF4E and not 4EHP. *Figure modified from Chapat et al. 2017(57).*

The results of the BioID assay and GO analysis data suggest C8Orf88 to be a novel interactor with eIF4E. 4EBPs have a well-characterized role in translational control and their dysregulation is implicated in diseases across nearly all tissue types. It is conceivable that C8Orf88 may have an uncharacterized role in translational regulation and disease as well. This work aims to characterize C8Orf88 and validate its interaction with eIF4E.

MATERIALS AND METHODS

Sequence Alignments

All genomic DNA sequences were obtained from the NCBI Gene database (149). Amino acid sequence of C8Orf88 was obtained using the ExPASy Translation Tool(150). Sequence alignments of C8Orf88 with the 4EBP homologs was performed using the Clustal Omega Multiple Sequence Alignment Tool(151).

Northern Blot Analysis

Mouse tissue RNA was obtained from Zyagen. RNA (4 μg) or ssRNA Ladder (New England Biolabs, NEB) was prepared to a volume of 20 μL with loading buffer (50% deionized formamide, 6% formaldehyde, 20 mM sodium borate, 0.2 mM $EDTA_{8.3}$). Samples were denatured at 65°C for 2 minutes directly prior to loading on a 1.2% agarose formaldehyde gel (6% formaldehyde, 20 mM sodium borate, 0.2 mM $EDTA_{8.3}$). The gel was run at 90V for 3 hours with buffer recirculation, after which the ssRNA Ladder (New England Biolabs, NEB) was cut from the gel and stained using SYBR™ Gold Nucleic Acid Gel Stain (Invitrogen) for one hour, as per manufacturer's instructions, followed by ultraviolet (UV) imaging. Samples were transferred to a Hybond N+ membrane (GE Healthcare) through capillary action in 10X SSC Buffer (1.5 M NaCl, 150 mM sodium citrate) at room temperature for 48 hours. The membrane was UV crosslinked using a Stratagene Stratalinker 2400 at a UV power of 1200.

The DNA probe was radiolabelled with α-^{32}P-dATP (Perkin Elmer) using the Takara Random Primer DNA Labeling Kit Ver.2.0 as per the manufacturer's instructions. Unincorporated α-^{32}P-dATP was removed by EZ-10 DNA spin column (Bio Basic). C8Orf88 probe was generated from the full-length protein coding region of the cDNA, isolated through restriction digest of plasmid pGEX-6p1-Flag-mC8Orf88 (kindly provided by Akiko Yanagiya). 18s rRNA probe was generated by PCR amplification of mouse tissue cDNA generated from mouse liver RNA using M-MuLV Reverse Transcriptase (New England Biolabs, NEB) with the following primers: 18s_rRNA_For, 5' – AACTGTGGTAATTCTAGAGC – 3', 18s_rRNA_Rev, 5' – CCATCGAAAGTTGATAGGGC – 3'. The membrane was blocked with 15mL hybridization buffer (50% formamide, 1X Denhardt's solution, 0.8 M NaCl, 4% D-SO_4, 1% sodium

pyrophosphate, 50 mM $Tris_{7.5}$, 0.5% SDS, 1mg/mL Salmon sperm DNA) at 42°C overnight in rotating hybridization oven. Following pre-hybridization, $15x10^6$ c.p.m. of denatured radiolabelled probe was added directly to the hybridization buffer and incubated at 42°C in a rotating hybridization oven for 16-24 hours. The membrane was washed twice each for 30 minutes with decreasing concentrations of SSC buffer (2X, 1X, 0.5X and 0.2X) and 0.1% SDS rotating at 65°C. Membranes were exposed at -80°C to X-ray film for 30 minutes (rRNA probe) and 4 days (C8Orf88 probe).

RT-qPCR

Mouse tissue RNA was obtained from Zyagen. cDNA was generated from RNA (1 μg) using M-MuLV Reverse Transcriptase (New England Biolabs, NEB). cDNA was diluted 1:10 and 1 μL was used in a 10 μL qPCR reaction using SsoFast EvaGreen Supermix (Bio-Rad) as per the manufacturer's instructions. Raw cycle threshold (Ct) values were compared to assess expression levels of the transcripts of interest.

Primers were designed using NCBI Primer-BLAST(152) and were obtained from Integrated DNA Technologies (IDT):

mC8Orf88_qPCR_For, 5' – TGGGTCTTGAGGCGTATG – 3'
mC8Orf88_qPCR_Rev, 5' – ATCTGCCCACTCCACTTTGT – 3'
m4EBP1_qPCR_For, 5' – ACTCACCTGTGGCCAAAACA – 3'
m4EBP1_qPCR_Rev, 5' – TTGTGACTCTTCACCGCCTG – 3'
m4EBP2_qPCR_For, 5' – TGTTGGACCGTCGCAATTCT – 3'
m4EBP2_qPCR_Rev, 5' – AAACTGAGCCTCATCCCCAAC – 3'
m4EBP3_qPCR_For, 5' – GGAGTGCAAGAACTCACCCA – 3'
m4EBP3_qPCR_Rev, 5' – TCAAACTGTTCGTCATCGGTT – 3'
B-actin_qPCR_For, 5' – TTCCTTCTTGGGTATGGAATCC – 3'
B-actin_qPCR_Rev, 5' – AGGAGCAATGATCTTGATCTTC – 3'

Plasmids and Recombinant Proteins

pLeGo-Flag-C8Orf88 and pLeGo-Flag-6aa-del-C8Orf88 were generated through restriction cloning of gBlocks™ Gene Fragments (Integrated DNA Technologies) into the pLeGo-SP6 backbone (obtained from Regina Cencic). pLeGo-Flag-4EBP[5A] was generated through PCR amplification of 4EBP[5A] from pCMV-4EBP[5A] (obtained from Francis Robert) using PCR primers contained a N-terminal Flag extension with the following primers:

Flag_4EBP[5A]_For, 5' – CCCCATATCATCGTGGGATCCCAATGGACTACAAGGACGAC

GACGATAAGATGTCGG – 3'

Flag_4EBP[5A]_Rev, 5' – CGAGATTTCACTGTTGAATTCTTAAAGTCCATCTCAAA – 3'

The PCR product was restriction cloned into the pLeGo-SP6 backbone.

pGEX-C8Orf88 and pGEX-6aadelC8Orf88 were generated through restriction cloning of gBlocks™ Gene Fragments (Integrated DNA Technologies) containing sequences codon optimized for *Escherichia coli* K12 into the pGEX-6P1 backbone (obtained from Regina Cencic). To generate recombinant GST-C8Orf88 and GST-6aa-del-C8Orf88, Rosetta™(DE3) Competent Cells (Sigma Aldrich) were transformed with pGEX-C8Orf88 and pGEX-6aadelC8Orf88, and induced with 0.5 mM IPTG for 3 hours at 37°C in a shaking incubator. A bacterial pellet was harvested via centrifugation, and a GST-based purification performed(153). GST-4EBP1 was obtained from Regina Cencic(154).

Cell Culture, Transfections and Lysate Preparation

HEK293T and HeLa cells were grown in Dulbecco's modified Eagle's medium (DMEM) supplemented with 10% bovine growth supplemented serum (BGSS), 1% penicillin-streptomycin antibiotics, and 2mM L-Glutamine at 37°C and 5% CO_2. Cells were maintained at sub-confluency. Cells were transiently transfected with pLeGo-Flag-C8Orf88, pLeGo-Flag-4EBP[5A], pLeGo-Flag-6aa-del-C8Orf88 or empty pLeGo plasmid DNA in a 6-well plate (3.5 μg) or 10cm dish (10 μg). Transfections were done using either polyethylenimine (PEI)(155) or calcium phosphate(156) as indicated.

Two methods of cell lysate preparation were utilized. Firstly, for NP40 lysis cells were washed once in ice cold PBS and scraped. Cells were then rinsed once in PBS and lyzed in 400µL NP40 lysis buffer (20 mM $Tris_{7.5}$, 150 mM NaCl, 0.5% NP40, 2mM $EDTA_{8.3}$) supplemented with protease inhibitors (2 μg/mL leupeptin, 10 μg/mL aprotinin, 2.5 μM pepstatin A) for 10 minutes on ice. Lysates were cleared of cellular debris via centrifugation. Secondly, for RIPA lysis cells were washed once in ice cold PBS and scraped. Cells were rinsed once in PBS and lyzed in 100µL RIPA lysis buffer (20 mM $Tris_{7.6}$, 100 mM NaCl, 1 mM $EDTA_{8.0}$, 1 mM $EGTA_{8.0}$, 1% NP-40, 0.5% deoxycholic acid, 0.1% SDS, 10 mM NaF, 20 mM β-glycerophosphate, 1 mM PMSF) supplemented with protease inhibitors (2 μg/mL leupeptin, 10 μg/mL aprotinin, 2.5 μM pepstatin A) for 10 minutes on ice. Lysates were cleared of cellular debris via centrifugation.

Western Blot Analysis

Samples were resolved on either 10% or 12.5% SDS-PAGE polyacrylamide gels and transferred to 0.2µm Immun-Blot™ PVDF Membrane (BIO-RAD). Membranes were blocked for 1 hour in 5% milk in Tris-buffered saline supplemented with 0.2% Tween 20 (TBS-T). The primary antibodies anti-DDDDK (Abcam) (recognizes FLAG-tag sequence), anti-eIF4E (Cell Signaling Technology) and anti-His (Cell Signaling Technologies) were diluted 1:1000 in 5% milk in TBS-T. The primary antibody anti-GST (Santa Cruz) was diluted 1:500 in 5% milk in TBS-T. Membranes were incubated with the primary antibody for 1 hour at room temperature and washed 3 times with TBS-T before addition of species-appropriate horseradish peroxidase (HRP) conjugated secondary antibody (Jackson ImmunoResearch) in 5% milk in TBS-T. Membranes were washed 3 times with TBS-T before addition of ECL UltraScence Western Substrate (FroggaBio) and exposed to Medical X-ray Blue film (Carestream).

***In vitro* Translation and Cap-affinity Chromatography**

Capped mRNAs were synthesized using SP6 RNA polymerase (New England Biolabs, NEB) from pLeGo-Flag-C8Orf88, pLeGo-Flag-4EBP[5A], pLeGo-Flag-6aa-del-C8Orf88 and pLeGo-Flag-eIF4E (obtained from Regina Cencic) in the presence of anti-reverse cap analog (ARCA)(157) and purified using a G50 Sephadex spin column. mRNAs encoding Flag-C8Orf88,

Flag-4EBP[5A] or Flag-6aa del C8Orf88 (0.5µg) were translated in conjunction with eIF4E (0.5µg) in wheat germ extract (Promega). Each mRNA pair was translated in a 30µL reaction for 1 hour at 25°C in the presence of 15.375µCi EasyTag™ L-[^{35}S]methionine (PerkinElmer). Translations were then subjected to cap-affinity chromatography using a γ-amino phenyl m^{7}GTP (C10 spacer) agarose (Jena Bioscience). Prior to use, beads were calibrated four times with LCB Buffer (20 mM Hepes$_{7.5}$, 0.1 M KCl, 0.2 mM EDTA). Translations were incubated on the resin for 2 hours at 4°C with end-over-end rotation. The resin was washed 3 times with LCB Buffer and 2 times with 500µM GTP before elution in 500µM m^{7}GTP(158). For each sample, the input, second GTP wash and m^{7}GTP elution were resolved on a 12.5% SDS-PAGE polyacrylamide gel which was then treated with EN^{3}HANCE™ (PerkinElmer) prior to drying and exposure to X-ray film (Carestream).

GST Pulldown

2.5µg of GST-C8Orf88, GST-4EBP1 or GST-6aa del C8Orf88 were incubated with 0.5µg His-eIF4E or His-eIF4E W73A in 50µL Binding Buffer (20mM Tris$_{7.5}$, 100mM KCl, 10% glycerol, 0.1% NP-40) for 1 hour at room temperature. 50µL of a 50% Glutathione Sepharose® 4 Fast Flow (Cytiva) slurry, washed 3 times with Binding Buffer, was added to the protein mix and incubated for 1 hour on ice. The beads were then washed 3 times with Binding Buffer prior to elution in 50µL 10mM Reduced Glutathione for 1 hour on ice. Proteins were resolved on a 10% SDS-PAGE and analyzed by Western blotting using anti-GST (Santa Cruz) and anti-His (Cell Signaling Technologies) antibodies.

Co-Immunoprecipitation and m^{7}GTP Cap-affinity Chromatography

In co-immunoprecipitation experiments, transiently transfected HEK293T cells (10cm dish) were lyzed in NP40 lysis buffer 24 hours post-transfection and cleared of cellular debris as previously described. Anti-FLAG® M2 magnetic beads (Millipore Sigma) were prepared by washing twice with NP40 lysis buffer. Lysates were immunoprecipitated with the antibody-coupled beads for 1 hour on ice and were periodically agitated to unsettle the beads which collected in the bottom of the tube. After immunoprecipitation, beads were washed 5 times with NP40 lysis

buffer and resuspended in 40µL 1X SDS loading buffer. Samples were resolved on a 12.5% SDS-PAGE and analyzed by Western blotting using anti-DDDDK (Abcam) and anti-eIF4E (Cell Signaling Technology) antibodies.

For m^7GTP cap-affinity chromatography, transfected HEK293T cells (10cm dish) were lyzed in 400µL NP40 lysis buffer 24 hours post-transfection as described previously. Lysates were then subjected to cap-affinity chromatography using a γ-amino phenyl m^7GTP (C10 spacer) agarose (Jena Bioscience), as described above. Samples were resolved on a 12.5% SDS-PAGE and analyzed by Western blotting using anti-DDDDK (Abcam) (recognizes FLAG-tag sequence) and anti-eIF4E (Cell Signaling Technology) antibodies.

RESULTS

Sequence alignment reveals homology between C8Orf88 and the 4EBP homologs.

The genomic sequence of human C8Orf88 was obtained from the NCBI Gene database (Gene ID: 100127983)(149). It is located on chromosome 8, cytoband q21.3, and its chromosomal location is 90958471 - 90985238 bp(159). Mapping of the coding sequence revealed 6 exons (Fig. 10A). The cDNA is 1323 nucleotides (nts) long, with a 5' UTR that is 433 nts in length, an open reading frame that is 354 nts in length, and a 3' UTR that is 536 nts in length. The open reading frame encodes a protein that is 177 amino acids in length with a predicted molecular weight of 13,372 Da. C8Orf88 shared between ~20-26% identity with the 4EBP homologs. Sequence alignment was done using the Clustal Omega Multiple Sequence Alignment Tool(151) (Fig. 10B). Importantly, the tyrosine (Y) and the leucine (L) of the canonical 4EBM sequence YXXXXLΦ were conserved in C8Orf88 (*grey highlight*, Fig. 10B), and two residues were conserved in the noncanonical 4EBM (*green box*, Fig. 10B). Two of the four conserved phosphorylation sites found in the 4EBP family were conserved in C8Orf88, with the first being T37 (in 4EBP1) and the second site having a conservative change of T46 (in 4EBP1) to serine in C8Orf88 (*asterisks*, Fig. 10B). The second conserved phosphorylation site contains a (Ser/Thr)-Pro motif (160).

A

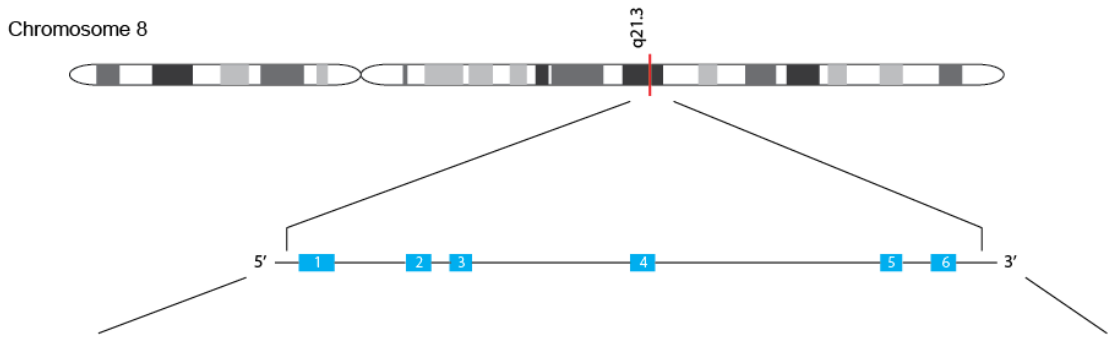


```
5′ AACGGTTCTACCCCGGCAGGGGTGCGGCTGCTCTCGAGGCTCAGCGCCCGAGGCCACGCCCCGCGCCCGCCCTGGGCCCG
CCTCGTGCCCCTCGGAGCCGCCTCCCGCCCCGCCCCCCGCCCCTCGCCCCCCGCCCCTCGCCCCCCGCCGCCGCCACCGCGGT
CAGCCAGCGGACCAGCGGCAGGAGCCGTTCCCCGACGGGCAGCAGGGCGCTCGGCCTCCGCGTGTGGGCTGAGCGCGGCGACG
CTGCTGCCCCGAAATCCCCGTGGATTTTGAGTCGGTAAGTGGCTAGGGAGGATGAGCGACACTGGGGGACGGAAGTCGGGCCC
CGTGGTGTGGAGGAGCGGGTGGGCGCCGTCTCCCAGGCCCGACCCCGGGAAAGTTGAGGCGAGGAAGAGAAGCTCTGAGTATG
GAACCTCAAAGTCTTTGGACA
ATG GAA ACA AAG AAA CTG ATC GGC AAA CCC CTT CAA CCT GCG AGG CCG GTT CGG CAC CTG ACA
 m   e   t   k   k   l   i   g   k   p   l   q   p   a   r   p   v   r   h   l   t

AGC CCG CCA GGG GCT GTT TTC CCG TTT AAC TTC CAG AAT GAA TAC CCC TGC AAC ACT CAG TGC
 s   p   p   g   a   v   f   p   f   n   f   q   n   e   y   p   c   n   t   q   c

ATC CAA AGC GGT GTC AGT AGA TGT AAG ACG AAC GGA ATG CAA GCG TTT TCT CAG GGA TTG AAC
 i   q   s   g   v   s   r   c   k   t   n   g   m   q   a   f   s   q   g   l   n

GAA CAG CAA CAG CAA CAG AGC CCA GTC AAG AAA GAA AGA ATC AAG TAT TCT AGA GAT TTC CTG
 e   q   q   q   q   q   s   p   v   k   k   e   r   i   k   y   s   r   d   f   l

CTC AAG CTG TCA TCC GTA TCT ATT TGT CGA AAG AAA CCC GAC TTT TTG CCA GAC CAT CCC ATC
 l   k   l   s   s   v   s   i   c   r   k   k   p   d   f   l   p   d   h   p   i

ATC GTG TTG CAA AAA CCC GAA AAT AAC CAA TCC TTT AAG
 i   v   l   q   k   p   e   n   n   q   s   f   k

CATTTTAAGAACAGATGAATTTAAGTTTGGACATCTGCAAATGAGGTGGATCTAGCAACAATAACTGTAATGGACTGTGACAA
TTCAATTTATTCTTAATTTTGATGGTTGGCTATTTGACTTCTCTAAAAATGAGAAAGAGCTATTTTAAAATATAAAGAATTTT
CTAATCAGTTTCAGCTTTGCAGGAGGTTTCCTGCATAAATTGGGAAGTAACACTGGAAAGTAGGAATTTGGTTAGTGAAGTGG
GAAGACTGTATATTTATAATTTGCATACTACTTGCAATTTTTTGTTTTTCATCACTTGTAATAATGGAATGGAAATGTAAGCT
GTAAAGACTCTCAAATATAAAATATTTGCTACAGTGTATATATGGTACATAATTGCTTGTTGCTTTTAAAGTTCCTTCTGTTG
TTCTGCTTCCCACTGATTTCATACCAGCTCATGAATGGATCATTACAGTCTCTCCAGAGGCTTAGAATGATTCAGAATGTTCA
ATGCATAGTTCTCAATAAACAGGAGGCAGAATTTTTAA 3′
```

B

```
C8ORF88     METKKLIGKPLQPARPVRHLTSPPGAVFPFNFQNEYPCNTQCIQSGVSRCKTNGMQAFSQ     60
4EBP1       MS-----GGSSCSQTPSRAIPATRRVVLGDGV----------QLPPGDYSTTPGGTLFS-     44
4EBP2       MS-----SSAGSGHQPSQSRAIPTRTVAISDA----------AQLPHDYCTTPGGTLFS-     44
4EBP3       ------------------MSTSTSCPIPGGR----------DQLPDCYSTTPGGTLYA-     30
                                                                  *

C8ORF88     GLNEQQQQQSPVKKERIKYSRDFLLKLSSVSICRKKPDFLPDHPIVLQKPENNQSFK---     117
4EBP1       ---------TTPGGTRIIYDRKFLMECRNSPVTKTPPRDLPTIPGVTSPSSDEPPMEASQ     95
4EBP2       ---------TTPGGTRIIYDRKFLLDRRNSPMAQTPPCHLPNIPGVTSPGTLIEDSKVEV     95
4EBP3       ---------TTPGGTRIIYDRKFLLECKNSPIARTPPCCLPQIPGVTTPPTAP-----L     75
                        *

C8ORF88     -------------------------       117
4EBP1       SHL--RNSPEDKRAGGEESQFEMDI       118
4EBP2       NNLNNLNNHDRKHAVGDDAQFEMDI       120
4EBP3       SKLEELKEQETEEEIPDDAQFEMDI       100
```

Figure 10. C8Orf88 cDNA sequence and amino acid sequence alignment with the 4EBP homologs. (A) Visualization of *C8Orf88*'s location on chromosome 8 (top), visualization of the unspliced C8Orf88 transcript with exons shown in blue (middle), and the cDNA sequence (bottom). (B) Sequence alignment of C8Orf88 with the three 4EBP homologs. Conserved sequences in 4EBPs involved with eIF4E binding activity are identified with boxes, consisting of the canonical 4EBM (red), the elbow loop domain (blue) and the non-canonical 4EBM (green). Tyrosine (Y) and leucine (L) of the canonical 4EBM sequence YXXXXLΦ are highlighted in grey. The two conserved phosphorylation sites are denoted with asterisks.

Mouse tissue RNA analysis maps C8Orf88 expression to testis.

To determine expression levels across different tissue types, Northern blot and real-time quantitative polymerase chain reaction (RT-qPCR) analysis of RNA isolated from mouse tissue was performed. A band of 900bp was detected via Northern blot for testis RNA when probed for C8Orf88, which is smaller than the predicted mRNA size of 1300bp (Fig. 11). No bands were detected for other tissues.

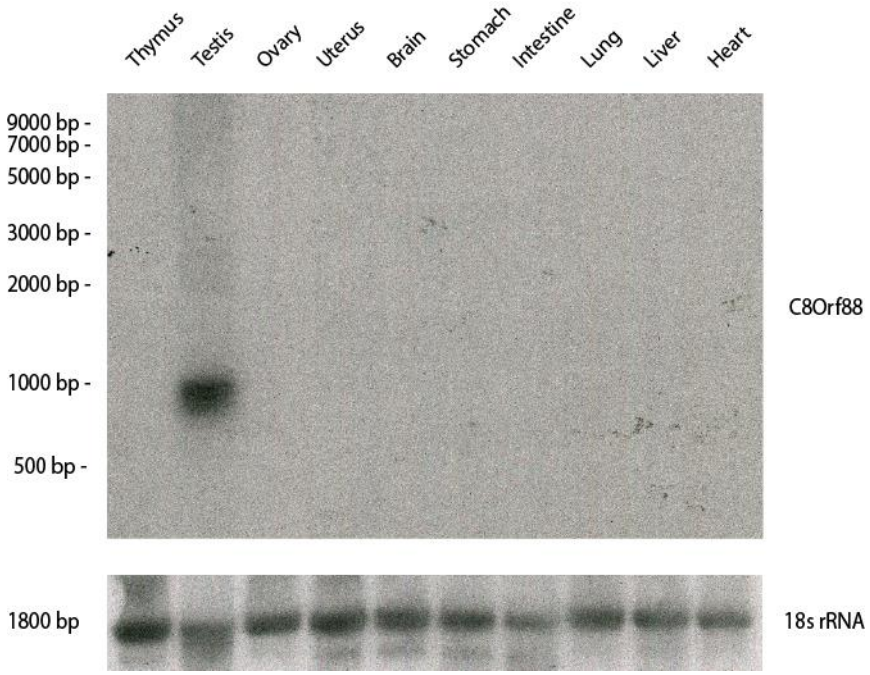

Figure 11. Northern blot analysis. Mouse tissue RNA obtained from Zyagen was used to assess tissue expression of C8Orf88.

RT-qPCR was performed using the same mouse tissue RNA used for the Northern blot analysis. C8Orf88 was detected at low levels across all tissue types (Fig. 12A). The highest Ct value for C8Orf88 amplification was detected in placenta at embryonic stage E11, suggesting lowest expression in this tissue type (Fig. 12A). The Ct values for testis C8Orf88 RNA were around 10 cycles lower than most other tissues, suggesting highest mRNA expression in this tissue (Fig. 12A). β-actin was detected at consistent levels across all tissue types, except skeletal muscle which showed a higher Ct value for both β-actin and C8Orf88 (Fig. 12A). When assessing mRNA levels of all three 4EBP family members and comparing them to C8Orf88, the greatest variance in expression levels of each mRNA between tissue types was seen in C8Orf88 compared to the three 4EBP family members (Fig. 12B). For all samples qPCR products were of the predicted sizes when analyzed on agarose gel (not shown).

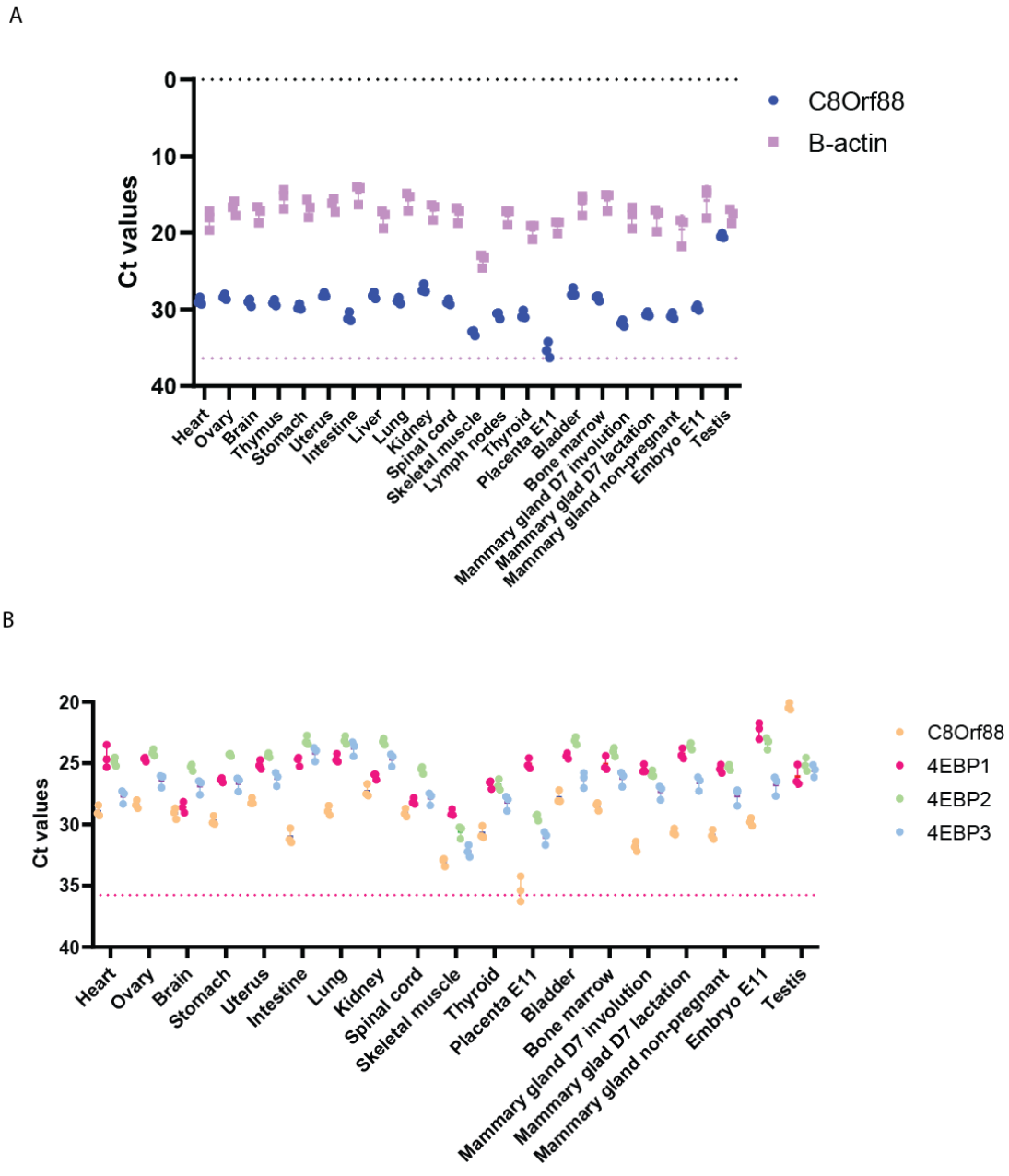

Figure 12. Testis shows greatest expression of C8Orf88 across mouse tissue RNA. (A) Ct values detected from C8Orf88 and B-actin amplification. The dotted pink line represents the Ct value of the water control for B-actin. (B) Ct values detected from the amplification of the three 4EBP homologs and C8Orf88. The dotted fuchsia line represents the Ct value of the water control for 4EBP1.

The expression profile observed in mouse tissue RNA was consistent with available RNA-seq data from 27 human tissues, which showed testis to have the highest C8Orf88 expression with a reads per kilobase million (RPKM) value of 47.21 ± 5.881 (N=7) (Fig. 13)(149,161). The second highest RPMK value was in the brain, being 23.47 ± 8.766 (N=3), and third being heart at 12.986 ± 2.617 (N=4) (Fig. 13)(149,161). RPMK values for all other tissues were less than 10 (Fig. 13)(149,161).

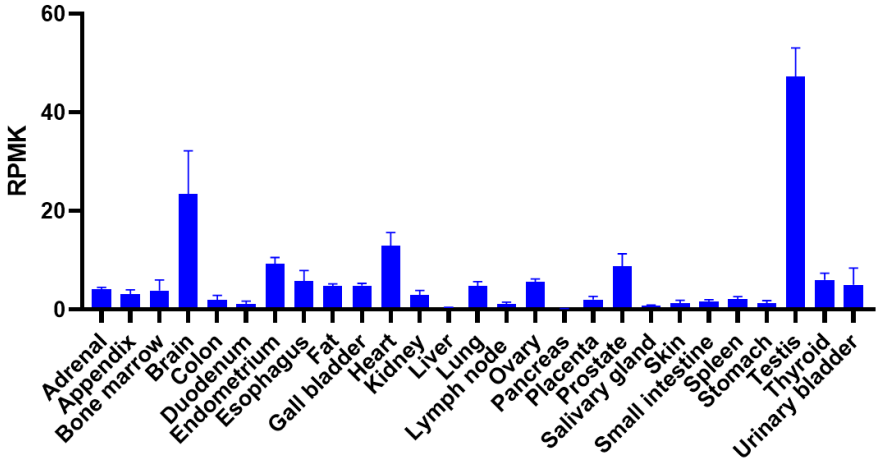

Figure 13. Available RNAseq data showing C8Orf88 expression levels in human tissue samples. Testis shows the greatest RNA levels of all samples with an RPMK value of 47.21 ± 5.881. The second highest expression levels are observed in brain, with an RPMK value of 23.47 ± 8.766. *Data obtained from NCBI Gene (147, 159).*

C8Orf88 interacts with eIF4E *in vitro*.

To investigate the interaction between C8Orf88 and eIF4E, recombinant tagged proteins were purified and used in a GST pulldown assay (Fig. 14A). GST-4EBP1 was used as a positive control, previously shown to interact with His-eIF4E in this assay(154). Additionally, a mutant C8Orf88 was generated containing a 6 amino acid deletion (6aa-del) in the canonical 4EBM which is expected to exert inhibitory effects on binding of eIF4E, and was included in the GST-pulldown experiments. However it should be noted that non-canonical 4EBMs have been observed to be sufficient for binding eIF4E *in vitro* (88), so some binding activity may be retained. Another mutant used in this assay was His-eIF4E W73A, which harbors a mutation in the conserved hydrophobic pocket on the dorsal surface of eIF4E which is necessary for interaction with the canonical 4EBM(43). All proteins were detected in the input lanes at comparable levels (*Input*, Fig. 14A). For the pulldowns, GST-4EBP1 showed interaction, though weak, with His-eIF4E as expected, while interaction with His-eIF4E W73A was not observed (*Lanes 6 and 7*, Fig. 14A). GST-C8Orf88 showed interaction with His-eIF4E as well as His-eIF4E W73A (*Lanes 8 and 10*, Fig. 14A). Lastly, GST-6aa-del-C8Orf88 did not notably interact with His-eIF4E (*Lane 9*, Fig. 14A).

ARCA-capped mRNAs encoding Flag-4EBP[5A], Flag-C8Orf88, Flag-6aa del C8Orf88 and eIF4E were synthesized *in vitro*. The 4EBP[5A] mutant is a nonphosphorylatable 4EBP1 mutant where the first five phosphorylation sites, T37, T46, S65, T70 and S83, are converted to alanine(162,163). Flag-4EBP[5A], Flag-C8Orf88 or Flag-6aa-del-C8Orf88 mRNAs were co-translated with eIF4E mRNAs in wheat germ extract in the presence of [^{35}S]methionine and subjected to cap-affinity chromatography. eIF4E bound the cap affinity resin as expected, as a band of the predicted size was detected in both input and m^{7}GTP lanes for all samples (*Lanes 3, 6 and 9*, Fig. 14B). As predicted, Flag-4EBP[5A] interacted with cap-bound eIF4E as a band of the predicted size was eluted from the column (*Lane 3*, Fig. 14B). Flag-C8Orf88 was also observed to interact with cap-bound eIF4E (*Lane 6*, Fig. 14B). Lastly, Flag-6aa-del-C8Orf88 did not interact with cap-bound eIF4E (*Lane 9*, Fig. 14B). These results indicate that *in vitro* C8Orf88 can interact with eIF4E and that the 4EBM is essential for this interaction.

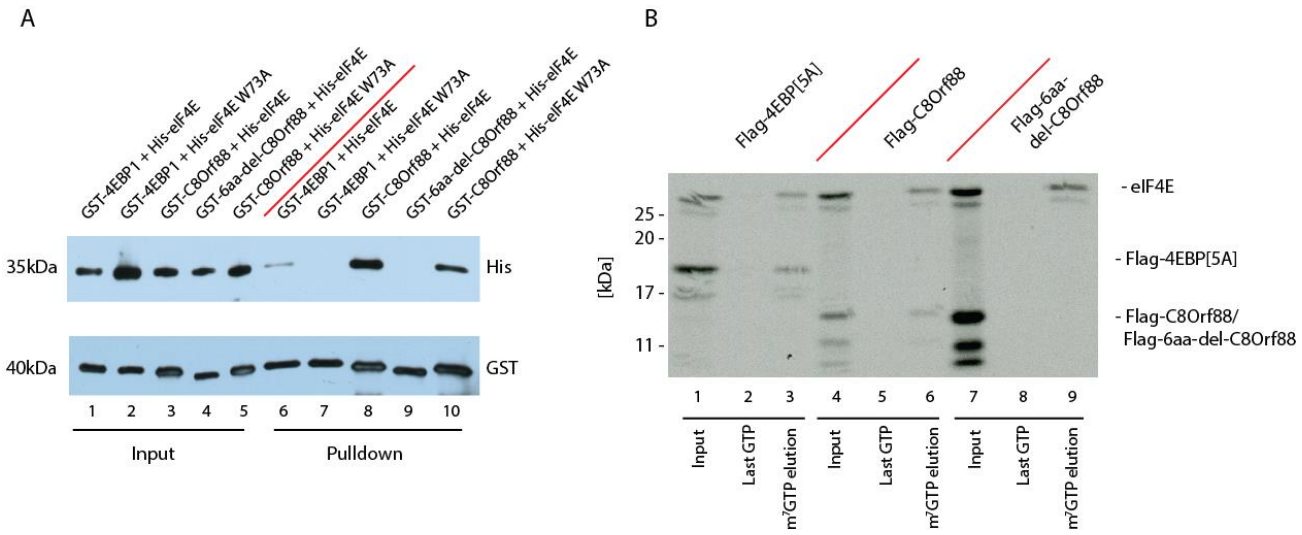

Figure 14. Interaction between C8Orf88 and eIF4E *in vitro*. (A) GST pulldown of GST-tagged C8Orf88, 4EBP1 and 6aa-del-C8Orf88 recombinant proteins in combination with His-4E or His-4E W73A. (B) Capped mRNAs were synthesized *in vitro* and translated in conjunction with eIF4E mRNA in wheat germ extract in the presence of ^{35}S-labelled methionine. Translations were incubated with an m^{7}GTP resin for cap-affinity chromatography. The resin was washed three times with LCB buffer and twice with 500µM GTP before elution in 500µM m^{7}GTP. For each translation, input, last GTP wash and the m^{7}GTP elution were resolved by SDS-PAGE and visualized using autoradiography.

C8Orf88 interacts with eIF4E in cells.

HEK293T cells were transiently transfected to express Flag-4EBP[5A], Flag-C8Orf88 or Flag-6aa-del-C8Orf88, and cells were harvested 24 hours after transfection. Cell lysates were subjected to immunoprecipitation using anti-Flag antibody conjugated magnetic beads (Fig. 15A). All Flag-tagged proteins and eIF4E were detected in the input lanes, confirming expression of these proteins (*Input*, Fig. 15A). Endogenous eIF4E co-immunoprecipitated with Flag-4EBP[5A] as expected, as well as with Flag-C8Orf88 (*Lanes 6 and 7*, Fig. 15A). Endogenous eIF4E did not co-immunoprecipitate from cells having received empty expression vector or expressing Flag-6aa-del-C8Orf88 (*Lanes 5 and 8*, Fig. 15A).

Secondly, HEK293T cells transiently transfected to express the same three Flag-tagged proteins were harvested 24 hours after transfection. Lysates were subjected to cap-affinity chromatography using m^7GTP-affinity chromatography (Fig. 15B). All Flag-tagged proteins and endogenous eIF4E were detected in the input lanes, confirming their expression in the lysates (*Lanes 1, 4 and 7*, Fig. 15B). eIF4E was eluted from the cap column for all samples, indicating it successfully bound the resin (*Lanes 3, 6 and 9*, Fig. 15B). Flag-4EBP[5A] was eluted from the column, suggesting an interaction with cap-bound eIF4E as expected (*Lane 6*, Fig. 15B). Flag-C8Orf88 was eluted from the column, also suggesting an interaction with cap-bound eIF4E (*Lane 3*, Fig. 15B). Flag-6aa-del-C8Orf88 did not elute from the column consistent with the importance of the 4EBM for eIF4E interaction (*Lane 9*, Fig. 15B).

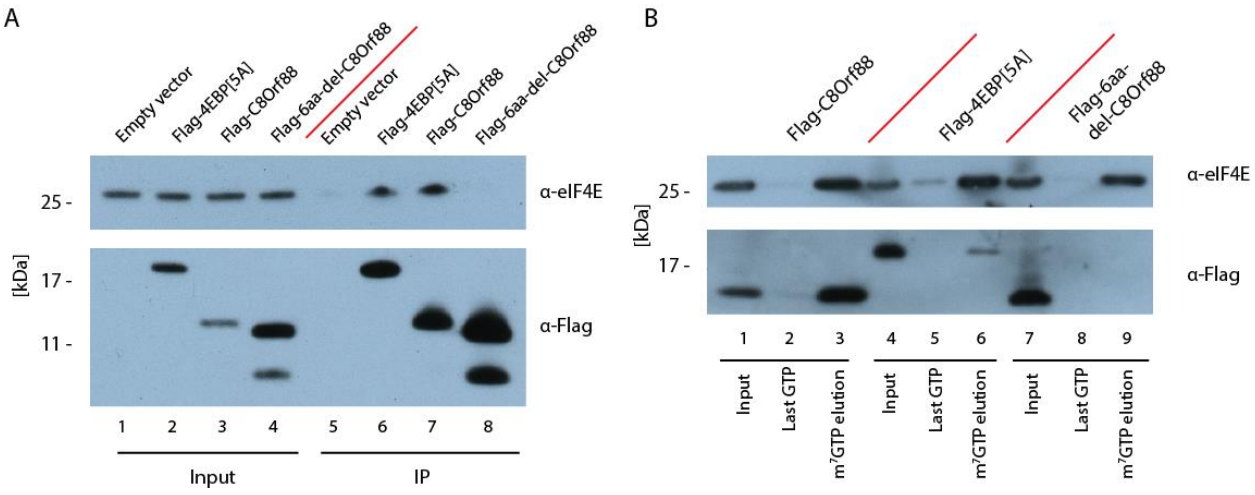

Figure 15. Interaction between C8Orf88 and eIF4E in cells. (A) Immunoprecipitation of transfected HEK293T cell lysates with anti-Flag antibody conjugated magnetic beads. Samples were resolved by SDS-PAGE and analyzed by Western blotting. (B) m^7GTP cap-affinity chromatography of transfected HEK293T cell lysates. The resin was washed three times with LCB buffer and twice with 500µM GTP before elution in 500µM m^7GTP. For each sample the input, last GTP wash and m^7GTP elution were resolved by SDS-PAGE and analyzed by Western blotting.

DISCUSSION

In our study, we have mapped the expression of C8Orf88 to testes in mice (Fig. 11 and 12). This expression pattern is congruent with RNA-seq data obtained from 27 human tissue samples, which also confirmed testis to show highest expression with an RPMK value of 47.21 ± 5.881 (N=7) (Fig. 13)(149,161). This study identified two other tissues that express C8Orf88 above baseline levels, being brain and heart with RPMK values of 23.47 ± 8.766 (N=3) and 12.986 ± 2.617 (N=4), respectively (Fig. 13)(149,161). RPMK values for all other tissues were less than 10 (Fig. 13)(149,161). Using Northern blot analysis and RT-qPCR of mouse tissue RNA, we were not able to detect C8Orf88 expression in brain and heart above what we observed to be the baseline expression across all mouse tissues sampled (Fig. 12). This discrepancy may be due to interspecies differences in gene expression patterns, or due to differences in sensitivities of the methods used as qPCR is less sensitive than RNAseq at detecting mRNAs with low abundance(164).

The conservation of tissue-specific expression of C8Orf88 in mice and humans implies it plays a functionally important and evolutionarily conserved role in testes. A meta-analysis of mouse and human microarray data revealed that genes expressed in a highly tissue-specific manner showed the highest degrees of expression pattern similarity across species(165). The study also found substantial overlap in tissue expression patterns of genes involved in basic cellular processes, such as protein synthesis(165). Conserved, tissue-specific expression in its relation to functional significance is further supported by the tissue-driven hypothesis, which states that important biological processes should be conserved, and that tissue-expression patterns of a gene might constrain the permissible variation in its expression(166). In other words, the more tissue-specific the expression of a certain gene is, the less likely it is to show variation in its expression between species(166). Together, this interspecies, tissue-specific conservation suggests that C8Orf88 has a physiologically significant role in testes. The relevance of the conservation of C8Orf88 expression in testes is further strengthened by the finding that testes have been found to have rapid interspecies expression divergence(166), meaning the expression of C8Orf88 has been conserved despite some of the highest incidents of tissue expression divergence in this tissue type.

Further narrowing its tissue-specific expression profile, C8Orf88 expression has been mapped to the germ cells of testes in The Human Protein Atlas(167). Specifically, RNA expression was enhanced in early spermatids, spermatocytes and late spermatids. When genes are clustered

according to their expression across samples, C8Orf88 expression was mapped to the "Spermatocytes – Spermatogenesis" cluster with the highest possible confidence score, indicative of a strong association. This cell-type specific mapping allows for speculation about the functional role of C8Orf88. Furthermore, tissue immunohistochemistry (IHC) of testes using a C8Orf88 antibody detected its expression at the protein level in spermatocytes(167). Translational control has been shown to be critical in the lifecycle of germ cells, with roles in stem cell maintenance, meiotic entry, completion of meiosis, and gamete differentiation(168,169). In particular, recruitment of selective messenger ribonucleoproteins (mRNPs) to ribosomes by eIF4 factors is recognized to play a vital role in translational control during development (170,171). During the development of oocytes and embryos, mRNP granules control gene expression through precise spatial-temporal regulation of mRNA expression(172). This careful gene regulation is essential for correct progression of the developmental program(172). It has been previously hypothesized that eIF4G dissociates 4EBPs from repressed mRNPs and activate their translation, driving progression through the stages of development(173). The identification of C8Orf88, a novel germ cell-specific 4EBP, may have important implications in translational control during spermatogenesis and development.

We were able to confirm that C8Orf88 interacts with eIF4E *in vitro* and in cells (Fig. 14 and 15). Using recombinant proteins, the interaction between C8Orf88 and eIF4E was validated *in vitro* (Fig. 14A). However, in this experiment an interaction between GST-C8Orf88 and His-eIF4E W73A was also observed, indicating that C8Orf88 can interact with eIF4E independently of the interaction between the canonical 4EBM and the dorsal surface of eIF4E (Fig. 14A). This is suggestive of the presence of a non-canonical 4EBM in C8Orf88, which has previously been noted to be sufficient for binding of 4EBPs to eIF4E *in vitro* (88). In this case we would expect GST-6aa-del-C8Orf88 (where the canonical 4EBM of C8Orf88 is mutated) to still be able to interact with eIF4E, however this was not observed (Fig. 14A). One possibility for this discrepancy could be due to the nature of the six amino acid deletion in C8Orf88, which might interfere with the protein's folding ability. This possibility is supported by the relatively low yields consistently obtained in the preparation of this recombinant protein (not shown). GST-4EBP1 showed a weaker interaction with His-eIF4E than did GST-C8Orf88 (Fig. 14A). While this discrepancy should be further investigated, it is possible that GST-C8Orf88 has a stronger affinity for eIF4E than GST-4EBP1. In contrasting GST-C8Orf88, GST-4EBP1 did not show an interaction with His-4E W73A

(Fig. 14A), consistent with previous experiments(174). A possible direction to investigate differences in affinity for eIF4E would be to undertake a time-synchronized fluorescence titration(50,175) of 4EBP1 and C8Orf88 with eIF4E to compare the kinetics of the interactions.

After validation of the interaction between eIF4E and C8Orf88 *in vitro*, the interaction was validated in cells using immunoprecipitation (Fig. 15A). Cells were transiently transfected to express Flag-tagged C8Orf88, 4EBP[5A], or 6aa-del-C8Orf88 and lysates were subjected to anti-Flag antibody immunoprecipitation. Endogenous eIF4E was found to co-immunoprecipitate with Flag-C8Orf88, suggesting an interaction between C8Orf88 and eIF4E in cells (Fig. 15A). Deletion of the canonical 4EBM in C8Orf88 abolished the interaction with eIF4E in cells (Fig. 15A). The presence of a second, smaller protein band in the Flag-6aa-del-C8Orf88 lane is observed for both input and immunoprecipitation (Fig. 15A). This is likely a truncated mutant C8Orf88 with an intact Flag-tag as it retains ability to immunoprecipitate. While *in vitro* data suggests the presence of a non-canonical 4EBM in C8Orf88 (Fig. 14A), we would not expect the non-canonical 4EBM to be sufficient for binding eIF4E in cells due to competitive factors. The sufficiency of non-canonical 4EBMs within 4EBPs to bind eIF4E has only been observed *in vitro* in previous studies(88), and the decrease in affinity for eIF4E upon deletion of the canonical 4EBM may render it unable to compete with endogenous eIF4G for the dorsal surface of eIF4E(95). The non-canonical 4EBM is thought to primarily be important for the docking of the 4EBPs. This competitive binding model of 4EBPs is described in Figure 16(88).

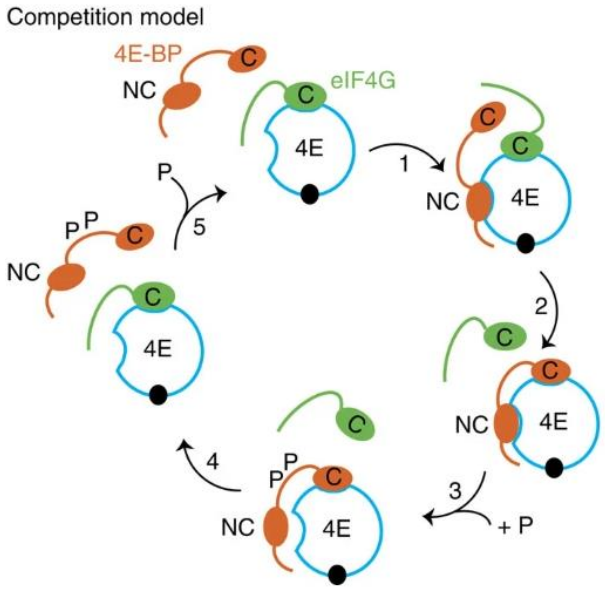

Figure 16. Competition model of 4EBPs with eIF4G for eIF4E. The non-canonical 4EBM is thought to be important for the docking of 4EBPs to the lateral surface of eIF4E (1). The canonical 4EBM is then primed to compete with eIF4G for the binding pocket on the dorsal surface of eIF4E (2). Phosphorylation of the 4EBPs, such as through mTORC1 activation, reduces the affinity of the 4EBP for eIF4E (3). In this state of reduced affinity, eIF4G can then outcompete 4EBP for binding to eIF4E (4). Figure obtained from *Igreja 2014(88)*.

C8Orf88 was observed to interact with cap-bound eIF4E *in vitro* and in cells (Fig. 14B and 15B). First, proteins were translated *in vitro* in wheat germ extract and subjected to m^7GTP cap-affinity chromatography. Flag-C8Orf88 was detected in the m^7GTP elution lane along with eIF4E (Fig. 14B). This suggests an interaction between C8Orf88 and cap-bound eIF4E. This activity is characteristic of 4EBPs and was predictably observed between Flag-4EBP[5A] and cap-bound eIF4E (Fig. 14B). This characteristic interaction was also observed in cells, where C8Orf88 eluted from the cap column in the m^7GTP elution (Fig. 15B). Elution of C8Orf88 from the resin in both cases implies that the interaction of C8Orf88 with eIF4E does not preclude eIF4E binding to the cap structure. The interaction observed between cap-bound eIF4E and C8Orf88 in cells is of particular interest as it shows C8Orf88 to be a competitor with other endogenously expressed 4EBPs. As previously mentioned, it would be of interest to compare the affinities of endogenous 4EBPs and C8Orf88 for eIF4E.

There are several avenues of investigation which could shed more light on the physiological relevance of C8Orf88. Here we confirm C8Orf88 to be a testes-specific 4EBP, which raises questions about its potential role in this tissue type. It is possible that C8Orf88 is the predominantly expressed 4EBP in testes. In contrast, 4EBP1 is predominantly expressed in skeletal muscle, pancreas and adipose tissue, whereas 4EBP2 is predominantly expressed in the brain and lymphocytes(86,87). It would be of interest to compare abundance of C8Orf88 with other 4EBPs to determine if it is the predominant 4EBP expressed in testes. To further characterize C8Orf88 as a 4EBP, its status as a phosphoprotein should be investigated. Confirming phosphorylation of C8Orf88 could provide insight on the regulatory mechanisms of this protein. Contingent on these results, it should then be determined whether C8Orf88 is a target of mTORC1. Targeting by mTORC1 is not a determinant of 4EBP activity, as 4EBP3 is not regulated by mTORC1 phosphorylation and rather is transcriptionally regulated(143), however it would be indicative of potential roles in malignancy.

Testicular cancer is the most common cancer found in men aged 14-44(176). Cancers with germ-cell origins, such as testicular seminomas, make up ~50% of all testicular cancer cases(177). Given the extensively characterized role of 4EBP1 dysregulation across many malignancies(113) and the mapping of C8Orf88 to the germ cells of testes(167), we can question whether C8Orf88 might play a role in tumorigenesis and disease progression of testicular cancers of germ cell origin. While the genetic origin of germ cell tumors (GCTs) is almost universally observed to be a gain of genetic material or internal rearrangement of chromosome 12p(178), mechanisms associated with other factors linked to disease progression and worse disease outcomes such as metastasis and chemoresistance are less defined. In a recent clinical whole-exome and transcriptome sequence study of GCTs, p53 was found to be expressed in all samples sequenced(179). This is a unique and unusual feature, as p53 is mutated in nearly half of solid tumors(180). Expression of p53 is though to be essential for cisplatin-induced apoptosis in GCTs(180). 4EBP activity has previously been linked to p53 expression in primary fibroblasts, where knock-down of 4EBP1 and 4EBP2 in conjunction with p53 expression led to resistance of oncogene-driven transformation and premature senescence(118). If C8Orf88 is a germ cell-specific 4EBP, it may play a role in senescence and apoptosis as governed by p53 in GCTs. Secondly, chemoresistance occurs in ~10% of testicular GCTs, and underlying mechanisms remain unclear(181). Whole exome sequencing and copy number analysis in platinum-resistant testicular GCTs reveals that there are multiple mutations involved with this chemoresistance(181). Characterization of a novel germ cell-specific 4EBP might elucidate one potential source of dysregulation leading to chemoresistance, as eIF4E overexpression has been previously implicated in drug resistance(83). To explore the role of C8Orf88 in GCTs, the NTera-2 human testicular embryonal carcinoma and F9 mouse teratocarcinoma cell lines can be utilized(182).

While we may speculate about a potential role for C8Orf88 as a 4EBP in the context of GCTs, prognostic data is already available from online databanks. Data available on the Human Protein Atlas has found a significant ($p<0.001$) association between C8Orf88 expression and patient survival in urothelial cancer and melanoma(167). Four hundred and six samples from urothelial cancer patients analyzed by The Cancer Genome Atlas(183) revealed high expression of C8Orf88 as an unfavourable prognostic marker in urothelial cancer. One hundred and two samples from melanoma patients revealed high C8Orf88 expression to be a poor prognostic marker

in this malignancy as well. This data provides rationale for characterizing the consequences of aberrant C8Orf88 expression in the context of these tissues.

Cytogenic abnormalities have been recorded at chromosome 8, cytogenic band q21.3, in congenital erythroleukemia(184), which is the chromosomal location of C8Orf88. The reported translocation is t(1;8)(p32;q21.3)/*RUNX1T1* split(184). Similar translocations, described t(1;8)(p22-p32;q22-q23), were found in cases of acute myeloid leukemia (AML) and non-Hodgkin lymphoma (NHL)(185). Chromosomal translocation events in a cancer context are causative of dysregulated expression of oncogenes or creation of fusion genes(186). While we cannot determine a relationship between C8Orf88 expression and these described chromosomal translocations, dysregulation or loss of a protein with eIF4E-binding capabilities could lead to eIF4E-overexpression driven transformation(72). Combined with the poor prognostic value associated with elevated C8Orf88 expression in melanomas and urothelial cancers, these chromosomal abnormalities may influence expression of C8Orf88 with relevance in the context of leukemia as well.

CONCLUSION

In conclusion, we characterized a novel testes-specific 4EBP. The interaction between C8Orf88 and eIF4E was confirmed *in vitro* and in cells. Furthermore, C8Orf88 was found to interact with cap-bound eIF4E both *in vitro* and in transiently transfected cell lysates by cap-affinity chromatography. C8Orf88 RNA expression was mapped to testes using Northern blot analysis and RT-qPCR. Further RNA-seq data available through public databases such as the Human Protein Atlas and The Cancer Genome Project reveal C8Orf88 expression to be germ-cell specific, which raises questions about the potential role of this novel 4EBP in the translational control of germ-cell related processes such as spermatogenesis and development, as well as germ-cell specific malignancies, such as GCTs. Data presented here in conjunction with the recognized importance of the 4EBPs in translational control provides rationale for further investigation about the physiological role of this protein.

REFERENCES

1. Rhoads RE, Joshi-Barve S, Rinker-Schaeffer C. Mechanism of action and regulation of protein synthesis initiation factor 4E: effects on mRNA discrimination, cellular growth rate, and oncogenesis. Prog Nucleic Acid Res Mol Biol **1993**;46:183-219
2. Buttgereit F, Brand MD. A hierarchy of ATP-consuming processes in mammalian cells. Biochem J **1995**;312:163-7
3. Pelletier J, Sonenberg N. The Organizing Principles of Eukaryotic Ribosome Recruitment. Annu Rev Biochem **2019**;88:307-35
4. De Benedetti A, Graff JR. eIF-4E expression and its role in malignancies and metastases. Oncogene **2004**;23:3189-99
5. Liu GY, Sabatini DM. mTOR at the nexus of nutrition, growth, ageing and disease. Nature Reviews Molecular Cell Biology **2020**;21:183-203
6. Pelletier J, Schmeing TM, Sonenberg N. The multifaceted eukaryotic cap structure. Wiley Interdiscip Rev RNA **2021**;12:e1636
7. Shen L, Pelletier J. General and Target-Specific DExD/H RNA Helicases in Eukaryotic Translation Initiation. Int J Mol Sci **2020**;21
8. Gu S, Jeon HM, Nam SW, Hong KY, Rahman MS, Lee JB, *et al.* The flip-flop configuration of the PABP-dimer leads to switching of the translation function. Nucleic Acids Res **2022**;50:306-21
9. Siddiqui N, Sonenberg N. Signalling to eIF4E in cancer. Biochem Soc Trans **2015**;43:763-72
10. Pelletier J, Sonenberg N. Internal initiation of translation of eukaryotic mRNA directed by a sequence derived from poliovirus RNA. Nature **1988**;334:320-5
11. Merrick WC, Pavitt GD. Protein Synthesis Initiation in Eukaryotic Cells. Cold Spring Harb Perspect Biol **2018**;10
12. Filbin ME, Kieft JS. Toward a structural understanding of IRES RNA function. Curr Opin Struct Biol **2009**;19:267-76
13. Weingarten-Gabbay S, Elias-Kirma S, Nir R, Gritsenko AA, Stern-Ginossar N, Yakhini Z, *et al.* Comparative genetics. Systematic discovery of cap-independent translation sequences in human and viral genomes. Science **2016**;351
14. Komar AA, Hatzoglou M. Cellular IRES-mediated translation: the war of ITAFs in pathophysiological states. Cell Cycle **2011**;10:229-40
15. Komar AA, Hatzoglou M. Internal ribosome entry sites in cellular mRNAs: mystery of their existence. J Biol Chem **2005**;280:23425-8
16. Hellen CU, Sarnow P. Internal ribosome entry sites in eukaryotic mRNA molecules. Genes Dev **2001**;15:1593-612
17. Leppek K, Das R, Barna M. Functional 5′ UTR mRNA structures in eukaryotic translation regulation and how to find them. Nature Reviews Molecular Cell Biology **2018**;19:158-74
18. Spriggs KA, Stoneley M, Bushell M, Willis AE. Re-programming of translation following cell stress allows IRES-mediated translation to predominate. Biol Cell **2008**;100:27-38
19. Holcik M, Sonenberg N. Translational control in stress and apoptosis. Nature Reviews Molecular Cell Biology **2005**;6:318-27

20. Robert F, Cencic R, Cai R, Schmeing TM, Pelletier J. RNA-tethering assay and eIF4G:eIF4A obligate dimer design uncovers multiple eIF4F functional complexes. Nucleic Acids Res **2020**;48:8562-75
21. Galicia-Vázquez G, Chu J, Pelletier J. eIF4AII is dispensable for miRNA-mediated gene silencing. RNA **2015**;21:1826-33
22. Sénéchal P, Robert F, Cencic R, Yanagiya A, Chu J, Sonenberg N, *et al.* Assessing eukaryotic initiation factor 4F subunit essentiality by CRISPR-induced gene ablation in the mouse. Cell Mol Life Sci **2021**;78:6709-19
23. Galicia-Vázquez G, Cencic R, Robert F, Agenor AQ, Pelletier J. A cellular response linking eIF4AI activity to eIF4AII transcription. RNA **2012**;18:1373-84
24. Kulak NA, Pichler G, Paron I, Nagaraj N, Mann M. Minimal, encapsulated proteomic-sample processing applied to copy-number estimation in eukaryotic cells. Nat Methods **2014**;11:319-24
25. Linder P, Jankowsky E. From unwinding to clamping — the DEAD box RNA helicase family. Nature Reviews Molecular Cell Biology **2011**;12:505-16
26. Feoktistova K, Tuvshintogs E, Do A, Fraser CS. Human eIF4E promotes mRNA restructuring by stimulating eIF4A helicase activity. Proc Natl Acad Sci U S A **2013**;110:13339-44
27. Rozovsky N, Butterworth AC, Moore MJ. Interactions between eIF4AI and its accessory factors eIF4B and eIF4H. RNA **2008**;14:2136-48
28. Rogers GW, Jr., Richter NJ, Lima WF, Merrick WC. Modulation of the helicase activity of eIF4A by eIF4B, eIF4H, and eIF4F. J Biol Chem **2001**;276:30914-22
29. Özeş AR, Feoktistova K, Avanzino BC, Fraser CS. Duplex unwinding and ATPase activities of the DEAD-box helicase eIF4A are coupled by eIF4G and eIF4B. J Mol Biol **2011**;412:674-87
30. Chu J, Zhang W, Cencic R, O'Connor PBF, Robert F, Devine WG, *et al.* Rocaglates Induce Gain-of-Function Alterations to eIF4A and eIF4F. Cell Rep **2020**;30:2481-8.e5
31. Prévôt D, Darlix JL, Ohlmann T. Conducting the initiation of protein synthesis: the role of eIF4G. Biol Cell **2003**;95:141-56
32. Imataka H, Gradi A, Sonenberg N. A newly identified N-terminal amino acid sequence of human eIF4G binds poly(A)-binding protein and functions in poly(A)-dependent translation. EMBO J **1998**;17:7480-9
33. Gallie DR. The cap and poly(A) tail function synergistically to regulate mRNA translational efficiency. Genes Dev **1991**;5:2108-16
34. Khong A, Parker R. mRNP architecture in translating and stress conditions reveals an ordered pathway of mRNP compaction. J Cell Biol **2018**;217:4124-40
35. Adivarahan S, Livingston N, Nicholson B, Rahman S, Wu B, Rissland OS, *et al.* Spatial Organization of Single mRNPs at Different Stages of the Gene Expression Pathway. Mol Cell **2018**;72:727-38.e5
36. Andrade MA, Petosa C, O'Donoghue SI, Müller CW, Bork P. Comparison of ARM and HEAT protein repeats. J Mol Biol **2001**;309:1-18
37. Boesen T, Mohammad SS, Pavitt GD, Andersen GR. Structure of the catalytic fragment of translation initiation factor 2B and identification of a critically important catalytic residue. J Biol Chem **2004**;279:10584-92

38. Korneeva NL, First EA, Benoit CA, Rhoads RE. Interaction between the NH2-terminal domain of eIF4A and the central domain of eIF4G modulates RNA-stimulated ATPase activity. J Biol Chem **2005**;280:1872-81
39. Hilbert M, Kebbel F, Gubaev A, Klostermeier D. eIF4G stimulates the activity of the DEAD box protein eIF4A by a conformational guidance mechanism. Nucleic Acids Res **2011**;39:2260-70
40. Yanagiya A, Svitkin YV, Shibata S, Mikami S, Imataka H, Sonenberg N. Requirement of RNA binding of mammalian eukaryotic translation initiation factor 4GI (eIF4GI) for efficient interaction of eIF4E with the mRNA cap. Mol Cell Biol **2009**;29:1661-9
41. Marcotrigiano J, Lomakin IB, Sonenberg N, Pestova TV, Hellen CU, Burley SK. A conserved HEAT domain within eIF4G directs assembly of the translation initiation machinery. Mol Cell **2001**;7:193-203
42. Waskiewicz AJ, Johnson JC, Penn B, Mahalingam M, Kimball SR, Cooper JA. Phosphorylation of the cap-binding protein eukaryotic translation initiation factor 4E by protein kinase Mnk1 in vivo. Mol Cell Biol **1999**;19:1871-80
43. Pyronnet S, Imataka H, Gingras AC, Fukunaga R, Hunter T, Sonenberg N. Human eukaryotic translation initiation factor 4G (eIF4G) recruits mnk1 to phosphorylate eIF4E. EMBO J **1999**;18:270-9
44. Scheper GC, van Kollenburg B, Hu J, Luo Y, Goss DJ, Proud CG. Phosphorylation of eukaryotic initiation factor 4E markedly reduces its affinity for capped mRNA. J Biol Chem **2002**;277:3303-9
45. Yamanaka S, Zhang XY, Maeda M, Miura K, Wang S, Farese RV, Jr., *et al.* Essential role of NAT1/p97/DAP5 in embryonic differentiation and the retinoic acid pathway. EMBO J **2000**;19:5533-41
46. Joshi B, Cameron A, Jagus R. Characterization of mammalian eIF4E-family members. Eur J Biochem **2004**;271:2189-203
47. Christie M, Igreja C. eIF4E-homologous protein (4EHP): a multifarious cap-binding protein. Febs j **2021**
48. Romagnoli A, D'Agostino M, Ardiccioni C, Maracci C, Motta S, La Teana A, *et al.* Control of the eIF4E activity: structural insights and pharmacological implications. Cell Mol Life Sci **2021**;78:6869-85
49. Matsuo H, Li H, McGuire AM, Fletcher CM, Gingras AC, Sonenberg N, *et al.* Structure of translation factor eIF4E bound to m7GDP and interaction with 4E-binding protein. Nat Struct Biol **1997**;4:717-24
50. Niedzwiecka A, Marcotrigiano J, Stepinski J, Jankowska-Anyszka M, Wyslouch-Cieszynska A, Dadlez M, *et al.* Biophysical studies of eIF4E cap-binding protein: recognition of mRNA 5' cap structure and synthetic fragments of eIF4G and 4E-BP1 proteins. J Mol Biol **2002**;319:615-35
51. Lazaris-Karatzas A, Montine KS, Sonenberg N. Malignant transformation by a eukaryotic initiation factor subunit that binds to mRNA 5' cap. Nature **1990**;345:544-7
52. Rousseau D, Kaspar R, Rosenwald I, Gehrke L, Sonenberg N. Translation initiation of ornithine decarboxylase and nucleocytoplasmic transport of cyclin D1 mRNA are increased in cells overexpressing eukaryotic initiation factor 4E. Proc Natl Acad Sci U S A **1996**;93:1065-70
53. Martineau Y, Azar R, Bousquet C, Pyronnet S. Anti-oncogenic potential of the eIF4E-binding proteins. Oncogene **2013**;32:671-7

54. Rom E, Kim HC, Gingras AC, Marcotrigiano J, Favre D, Olsen H, *et al.* Cloning and characterization of 4EHP, a novel mammalian eIF4E-related cap-binding protein. J Biol Chem **1998**;273:13104-9
55. Wilhelm M, Schlegl J, Hahne H, Gholami AM, Lieberenz M, Savitski MM, *et al.* Mass-spectrometry-based draft of the human proteome. Nature **2014**;509:582-7
56. Zuberek J, Kubacka D, Jablonowska A, Jemielity J, Stepinski J, Sonenberg N, *et al.* Weak binding affinity of human 4EHP for mRNA cap analogs. RNA **2007**;13:691-7
57. Chapat C, Jafarnejad SM, Matta-Camacho E, Hesketh GG, Gelbart IA, Attig J, *et al.* Cap-binding protein 4EHP effects translation silencing by microRNAs. Proc Natl Acad Sci U S A **2017**;114:5425-30
58. Osborne MJ, Volpon L, Kornblatt JA, Culjkovic-Kraljacic B, Baguet A, Borden KL. eIF4E3 acts as a tumor suppressor by utilizing an atypical mode of methyl-7-guanosine cap recognition. Proc Natl Acad Sci U S A **2013**;110:3877-82
59. Bhat M, Robichaud N, Hulea L, Sonenberg N, Pelletier J, Topisirovic I. Targeting the translation machinery in cancer. Nat Rev Drug Discov **2015**;14:261-78
60. Rosenwald IB, Rhoads DB, Callanan LD, Isselbacher KJ, Schmidt EV. Increased expression of eukaryotic translation initiation factors eIF-4E and eIF-2 alpha in response to growth induction by c-myc. Proc Natl Acad Sci U S A **1993**;90:6175-8
61. Mao X, Green JM, Safer B, Lindsten T, Frederickson RM, Miyamoto S, *et al.* Regulation of translation initiation factor gene expression during human T cell activation. J Biol Chem **1992**;267:20444-50
62. Haydon MS, Googe JD, Sorrells DS, Ghali GE, Li BD. Progression of eIF4e gene amplification and overexpression in benign and malignant tumors of the head and neck. Cancer **2000**;88:2803-10
63. Bar-Peled L, Sabatini DM. Regulation of mTORC1 by amino acids. Trends Cell Biol **2014**;24:400-6
64. Laplante M, Sabatini David M. mTOR Signaling in Growth Control and Disease. Cell **2012**;149:274-93
65. Saxton RA, Sabatini DM. mTOR Signaling in Growth, Metabolism, and Disease. Cell **2017**;168:960-76
66. Hay N, Sonenberg N. Upstream and downstream of mTOR. Genes Dev **2004**;18:1926-45
67. Gingras AC, Raught B, Gygi SP, Niedzwiecka A, Miron M, Burley SK, *et al.* Hierarchical phosphorylation of the translation inhibitor 4E-BP1. Genes Dev **2001**;15:2852-64
68. Gingras AC, Kennedy SG, O'Leary MA, Sonenberg N, Hay N. 4E-BP1, a repressor of mRNA translation, is phosphorylated and inactivated by the Akt(PKB) signaling pathway. Genes Dev **1998**;12:502-13
69. Raught B, Gingras AC. eIF4E activity is regulated at multiple levels. Int J Biochem Cell Biol **1999**;31:43-57
70. Walsh D, Mohr I. Coupling 40S ribosome recruitment to modification of a cap-binding initiation factor by eIF3 subunit e. Genes Dev **2014**;28:835-40
71. Furic L, Rong L, Larsson O, Koumakpayi IH, Yoshida K, Brueschke A, *et al.* eIF4E phosphorylation promotes tumorigenesis and is associated with prostate cancer progression. Proceedings of the National Academy of Sciences **2010**;107:14134
72. Wendel HG, Silva RL, Malina A, Mills JR, Zhu H, Ueda T, *et al.* Dissecting eIF4E action in tumorigenesis. Genes Dev **2007**;21:3232-7

73. Graff JR, Konicek BW, Carter JH, Marcusson EG. Targeting the Eukaryotic Translation Initiation Factor 4E for Cancer Therapy. Cancer Res **2008**;68:631
74. Koch G, Bilello JA, Kruppa J, Koch F, Oppermann H. Amplification of translational control by membrane-mediated events: a pleiotropic effect on cellular and viral gene expression. Ann N Y Acad Sci **1980**;339:280-306
75. Koromilas AE, Lazaris-Karatzas A, Sonenberg N. mRNAs containing extensive secondary structure in their 5' non-coding region translate efficiently in cells overexpressing initiation factor eIF-4E. EMBO J **1992**;11:4153-8
76. Kevil CG, De Benedetti A, Payne DK, Coe LL, Laroux FS, Alexander JS. Translational regulation of vascular permeability factor by eukaryotic initiation factor 4E: implications for tumor angiogenesis. Int J Cancer **1996**;65:785-90
77. Fagan RJ, Lazaris-Karatzas A, Sonenberg N, Rozen R. Translational control of ornithine aminotransferase. Modulation by initiation factor eIF-4E. J Biol Chem **1991**;266:16518-23
78. Lazaris-Karatzas A, Sonenberg N. The mRNA 5' cap-binding protein, eIF-4E, cooperates with v-myc or E1A in the transformation of primary rodent fibroblasts. Mol Cell Biol **1992**;12:1234-8
79. Ruggero D, Montanaro L, Ma L, Xu W, Londei P, Cordon-Cardo C, *et al.* The translation factor eIF-4E promotes tumor formation and cooperates with c-Myc in lymphomagenesis. Nat Med **2004**;10:484-6
80. Zimmer SG, DeBenedetti A, Graff JR. Translational control of malignancy: the mRNA cap-binding protein, eIF-4E, as a central regulator of tumor formation, growth, invasion and metastasis. Anticancer Res **2000**;20:1343-51
81. Lazaris-Karatzas A, Smith MR, Frederickson RM, Jaramillo ML, Liu YL, Kung HF, *et al.* Ras mediates translation initiation factor 4E-induced malignant transformation. Genes Dev **1992**;6:1631-42
82. Li S, Perlman DM, Peterson MS, Burrichter D, Avdulov S, Polunovsky VA, *et al.* Translation initiation factor 4E blocks endoplasmic reticulum-mediated apoptosis. J Biol Chem **2004**;279:21312-7
83. Wendel HG, De Stanchina E, Fridman JS, Malina A, Ray S, Kogan S, *et al.* Survival signalling by Akt and eIF4E in oncogenesis and cancer therapy. Nature **2004**;428:332-7
84. Poulin F, Gingras AC, Olsen H, Chevalier S, Sonenberg N. 4E-BP3, a new member of the eukaryotic initiation factor 4E-binding protein family. J Biol Chem **1998**;273:14002-7
85. Pause A, Belsham GJ, Gingras AC, Donzé O, Lin TA, Lawrence JC, Jr., *et al.* Insulin-dependent stimulation of protein synthesis by phosphorylation of a regulator of 5'-cap function. Nature **1994**;371:762-7
86. Tsukiyama-Kohara K, Poulin F, Kohara M, DeMaria CT, Cheng A, Wu Z, *et al.* Adipose tissue reduction in mice lacking the translational inhibitor 4E-BP1. Nat Med **2001**;7:1128-32
87. Bidinosti M, Ran I, Sanchez-Carbente MR, Martineau Y, Gingras AC, Gkogkas C, *et al.* Postnatal deamidation of 4E-BP2 in brain enhances its association with raptor and alters kinetics of excitatory synaptic transmission. Mol Cell **2010**;37:797-808
88. Igreja C, Peter D, Weiler C, Izaurralde E. 4E-BPs require non-canonical 4E-binding motifs and a lateral surface of eIF4E to repress translation. Nat Commun **2014**;5:4790

89. Mader S, Lee H, Pause A, Sonenberg N. The translation initiation factor eIF-4E binds to a common motif shared by the translation factor eIF-4 gamma and the translational repressors 4E-binding proteins. Mol Cell Biol **1995**;15:4990-7
90. Marcotrigiano J, Gingras AC, Sonenberg N, Burley SK. Cap-dependent translation initiation in eukaryotes is regulated by a molecular mimic of eIF4G. Mol Cell **1999**;3:707-16
91. Peter D, Igreja C, Weber R, Wohlbold L, Weiler C, Ebertsch L, *et al.* Molecular architecture of 4E-BP translational inhibitors bound to eIF4E. Mol Cell **2015**;57:1074-87
92. Kinkelin K, Veith K, Grünwald M, Bono F. Crystal structure of a minimal eIF4E-Cup complex reveals a general mechanism of eIF4E regulation in translational repression. RNA **2012**;18:1624-34
93. Gosselin P, Oulhen N, Jam M, Ronzca J, Cormier P, Czjzek M, *et al.* The translational repressor 4E-BP called to order by eIF4E: new structural insights by SAXS. Nucleic Acids Res **2011**;39:3496-503
94. Lukhele S, Bah A, Lin H, Sonenberg N, Forman-Kay JD. Interaction of the eukaryotic initiation factor 4E with 4E-BP2 at a dynamic bipartite interface. Structure **2013**;21:2186-96
95. Paku Keum S, Umenaga Y, Usui T, Fukuyo A, Mizuno A, In Y, *et al.* A conserved motif within the flexible C-terminus of the translational regulator 4E-BP is required for tight binding to the mRNA cap-binding protein eIF4E. Biochem J **2011**;441:237-45
96. Mészáros B, Tompa P, Simon I, Dosztányi Z. Molecular principles of the interactions of disordered proteins. J Mol Biol **2007**;372:549-61
97. Bah A, Vernon RM, Siddiqui Z, Krzeminski M, Muhandiram R, Zhao C, *et al.* Folding of an intrinsically disordered protein by phosphorylation as a regulatory switch. Nature **2015**;519:106-9
98. Gingras AC, Gygi SP, Raught B, Polakiewicz RD, Abraham RT, Hoekstra MF, *et al.* Regulation of 4E-BP1 phosphorylation: a novel two-step mechanism. Genes Dev **1999**;13:1422-37
99. Roux PP, Topisirovic I. Regulation of mRNA translation by signaling pathways. Cold Spring Harb Perspect Biol **2012**;4
100. Beretta L, Gingras AC, Svitkin YV, Hall MN, Sonenberg N. Rapamycin blocks the phosphorylation of 4E-BP1 and inhibits cap-dependent initiation of translation. EMBO J **1996**;15:658-64
101. Sonenberg N, Gingras AC. The mRNA 5' cap-binding protein eIF4E and control of cell growth. Curr Opin Cell Biol **1998**;10:268-75
102. Kleijn M, Scheper GC, Voorma HO, Thomas AA. Regulation of translation initiation factors by signal transduction. Eur J Biochem **1998**;253:531-44
103. Gingras AC, Svitkin Y, Belsham GJ, Pause A, Sonenberg N. Activation of the translational suppressor 4E-BP1 following infection with encephalomyocarditis virus and poliovirus. Proc Natl Acad Sci U S A **1996**;93:5578-83
104. Kleijn M, Scheper GC, Wilson ML, Tee AR, Proud CG. Localisation and regulation of the eIF4E-binding protein 4E-BP3. FEBS Lett **2002**;532:319-23
105. Fadden P, Haystead TA, Lawrence JC, Jr. Identification of phosphorylation sites in the translational regulator, PHAS-I, that are controlled by insulin and rapamycin in rat adipocytes. J Biol Chem **1997**;272:10240-7

106. Heesom KJ, Avison MB, Diggle TA, Denton RM. Insulin-stimulated kinase from rat fat cells that phosphorylates initiation factor 4E-binding protein 1 on the rapamycin-insensitive site (serine-111). Biochem J **1998**;336 (Pt 1):39-48
107. Hara K, Yonezawa K, Kozlowski MT, Sugimoto T, Andrabi K, Weng QP, *et al.* Regulation of eIF-4E BP1 phosphorylation by mTOR. J Biol Chem **1997**;272:26457-63
108. Wang X, Li W, Parra JL, Beugnet A, Proud CG. The C terminus of initiation factor 4E-binding protein 1 contains multiple regulatory features that influence its function and phosphorylation. Mol Cell Biol **2003**;23:1546-57
109. Gingras AC, Raught B, Gygi SP, Niedzwiecka A, Miron M, Burley SK, *et al.* Hierarchical phosphorylation of the translation inhibitor 4E-BP1. Genes Dev **2001**;15:2852-64
110. Heesom KJ, Denton RM. Dissociation of the eukaryotic initiation factor-4E/4E-BP1 complex involves phosphorylation of 4E-BP1 by an mTOR-associated kinase. FEBS Lett **1999**;457:489-93
111. Rousseau D, Gingras AC, Pause A, Sonenberg N. The eIF4E-binding proteins 1 and 2 are negative regulators of cell growth. Oncogene **1996**;13:2415-20
112. Polunovsky VA, Gingras AC, Sonenberg N, Peterson M, Tan A, Rubins JB, *et al.* Translational control of the antiapoptotic function of Ras. J Biol Chem **2000**;275:24776-80
113. Musa J, Orth MF, Dallmayer M, Baldauf M, Pardo C, Rotblat B, *et al.* Eukaryotic initiation factor 4E-binding protein 1 (4E-BP1): a master regulator of mRNA translation involved in tumorigenesis. Oncogene **2016**;35:4675-88
114. Braun-Dullaeus RC, Mann MJ, Seay U, Zhang L, von Der Leyen HE, Morris RE, *et al.* Cell cycle protein expression in vascular smooth muscle cells in vitro and in vivo is regulated through phosphatidylinositol 3-kinase and mammalian target of rapamycin. Arterioscler Thromb Vasc Biol **2001**;21:1152-8
115. Fingar DC, Richardson CJ, Tee AR, Cheatham L, Tsou C, Blenis J. mTOR controls cell cycle progression through its cell growth effectors S6K1 and 4E-BP1/eukaryotic translation initiation factor 4E. Mol Cell Biol **2004**;24:200-16
116. Fingar DC, Salama S, Tsou C, Harlow E, Blenis J. Mammalian cell size is controlled by mTOR and its downstream targets S6K1 and 4EBP1/eIF4E. Genes Dev **2002**;16:1472-87
117. Liu J, Zhang C, Hu W, Feng Z. Tumor suppressor p53 and metabolism. J Mol Cell Biol **2019**;11:284-92
118. Petroulakis E, Parsyan A, Dowling RJ, LeBacquer O, Martineau Y, Bidinosti M, *et al.* p53-dependent translational control of senescence and transformation via 4E-BPs. Cancer Cell **2009**;16:439-46
119. Braunstein S, Karpisheva K, Pola C, Goldberg J, Hochman T, Yee H, *et al.* A hypoxia-controlled cap-dependent to cap-independent translation switch in breast cancer. Mol Cell **2007**;28:501-12
120. Dubois L, Magagnin MG, Cleven AH, Weppler SA, Grenacher B, Landuyt W, *et al.* Inhibition of 4E-BP1 sensitizes U87 glioblastoma xenograft tumors to irradiation by decreasing hypoxia tolerance. Int J Radiat Oncol Biol Phys **2009**;73:1219-27
121. Karlsson E, Pérez-Tenorio G, Amin R, Bostner J, Skoog L, Fornander T, *et al.* The mTOR effectors 4EBP1 and S6K2 are frequently coexpressed, and associated with a poor prognosis and endocrine resistance in breast cancer: a retrospective study including

patients from the randomised Stockholm tamoxifen trials. Breast Cancer Res **2013**;15:R96
122. Karlsson E, Waltersson MA, Bostner J, Pérez-Tenorio G, Olsson B, Hallbeck AL, *et al.* High-resolution genomic analysis of the 11q13 amplicon in breast cancers identifies synergy with 8p12 amplification, involving the mTOR targets S6K2 and 4EBP1. Genes Chromosomes Cancer **2011**;50:775-87
123. Nemes K, Sebestyén A, Márk A, Hajdu M, Kenessey I, Sticz T, *et al.* Mammalian target of rapamycin (mTOR) activity dependent phospho-protein expression in childhood acute lymphoblastic leukemia (ALL). PLoS One **2013**;8:e59335
124. Chen W, Drakos E, Grammatikakis I, Schlette EJ, Li J, Leventaki V, *et al.* mTOR signaling is activated by FLT3 kinase and promotes survival of FLT3-mutated acute myeloid leukemia cells. Mol Cancer **2010**;9:292
125. Schultz L, Albadine R, Hicks J, Jadallah S, DeMarzo AM, Chen YB, *et al.* Expression status and prognostic significance of mammalian target of rapamycin pathway members in urothelial carcinoma of urinary bladder after cystectomy. Cancer **2010**;116:5517-26
126. Rojo F, Najera L, Lirola J, Jiménez J, Guzmán M, Sabadell MD, *et al.* 4E-binding protein 1, a cell signaling hallmark in breast cancer that correlates with pathologic grade and prognosis. Clin Cancer Res **2007**;13:81-9
127. Zhang YJ, Dai Q, Sun DF, Xiong H, Tian XQ, Gao FH, *et al.* mTOR signaling pathway is a target for the treatment of colorectal cancer. Ann Surg Oncol **2009**;16:2617-28
128. Rice LW, Stone RL, Xu M, Galgano M, Stoler MH, Everett EN, *et al.* Biologic targets for therapeutic intervention in endometrioid endometrial adenocarcinoma and malignant mixed müllerian tumors. Am J Obstet Gynecol **2006**;194:1119-26; discussion 26-8
129. Salehi Z, Mashayekhi F. Expression of the eukaryotic translation initiation factor 4E (eIF4E) and 4E-BP1 in esophageal cancer. Clin Biochem **2006**;39:404-9
130. Jiao X, Pan J, Qian J, Luo T, Wang Z, Yu G, *et al.* Overexpression of p-4ebp1 in Chinese gastric cancer patients and its correlation with prognosis. Hepatogastroenterology **2013**;60:921-6
131. Mueller S, Phillips J, Onar-Thomas A, Romero E, Zheng S, Wiencke JK, *et al.* PTEN promoter methylation and activation of the PI3K/Akt/mTOR pathway in pediatric gliomas and influence on clinical outcome. Neuro Oncol **2012**;14:1146-52
132. Clark C, Shah S, Herman-Ferdinandez L, Ekshyyan O, Abreo F, Rong X, *et al.* Teasing out the best molecular marker in the AKT/mTOR pathway in head and neck squamous cell cancer patients. Laryngoscope **2010**;120:1159-65
133. Lee HW, Lee EH, Lee JH, Kim JE, Kim SH, Kim TG, *et al.* Prognostic significance of phosphorylated 4E-binding protein 1 in non-small cell lung cancer. Int J Clin Exp Pathol **2015**;8:3955-62
134. Iżycka-Świeszewska E, Drożyńska E, Rzepko R, Kobierska-Gulida G, Grajkowska W, Perek D, *et al.* Analysis of PI3K/AKT/mTOR signalling pathway in high risk neuroblastic tumours. Pol J Pathol **2010**;61:192-8
135. Castellvi J, Garcia A, Rojo F, Ruiz-Marcellan C, Gil A, Baselga J, *et al.* Phosphorylated 4E binding protein 1: a hallmark of cell signaling that correlates with survival in ovarian cancer. Cancer **2006**;107:1801-11
136. Graff JR, Konicek BW, Lynch RL, Dumstorf CA, Dowless MS, McNulty AM, *et al.* eIF4E activation is commonly elevated in advanced human prostate cancers and significantly related to reduced patient survival. Cancer Res **2009**;69:3866-73

137. Banko JL, Poulin F, Hou L, DeMaria CT, Sonenberg N, Klann E. The translation repressor 4E-BP2 is critical for eIF4F complex formation, synaptic plasticity, and memory in the hippocampus. J Neurosci **2005**;25:9581-90
138. Wiebe S, Nagpal A, Truong VT, Park J, Skalecka A, He AJ, *et al.* Inhibitory interneurons mediate autism-associated behaviors via 4E-BP2. Proc Natl Acad Sci U S A **2019**;116:18060-7
139. Gkogkas CG, Khoutorsky A, Ran I, Rampakakis E, Nevarko T, Weatherill DB, *et al.* Autism-related deficits via dysregulated eIF4E-dependent translational control. Nature **2013**;493:371-7
140. Santini E, Klann E. Reciprocal signaling between translational control pathways and synaptic proteins in autism spectrum disorders. Sci Signal **2014**;7:re10
141. Hooshmandi M, Truong VT, Fields E, Thomas RE, Wong C, Sharma V, *et al.* 4E-BP2-dependent translation in cerebellar Purkinje cells controls spatial memory but not autism-like behaviors. Cell Rep **2021**;35:109036
142. Tsukumo Y, Sonenberg N, Alain T. Transcriptional induction of 4E-BP3 prolongs translation repression. Cell Cycle **2016**;15:3325-6
143. Tsukumo Y, Alain T, Fonseca BD, Nadon R, Sonenberg N. Translation control during prolonged mTORC1 inhibition mediated by 4E-BP3. Nat Commun **2016**;7:11776
144. Martina JA, Diab HI, Lishu L, Jeong AL, Patange S, Raben N, *et al.* The nutrient-responsive transcription factor TFE3 promotes autophagy, lysosomal biogenesis, and clearance of cellular debris. Sci Signal **2014**;7:ra9
145. Roczniak-Ferguson A, Petit CS, Froehlich F, Qian S, Ky J, Angarola B, *et al.* The transcription factor TFEB links mTORC1 signaling to transcriptional control of lysosome homeostasis. Sci Signal **2012**;5:ra42
146. Roux KJ, Kim DI, Burke B, May DG. BioID: A Screen for Protein-Protein Interactions. Curr Protoc Protein Sci **2018**;91:19.23.1-19.23.15
147. Welsby I, Hutin D, Gueydan C, Kruys V, Rongvaux A, Leo O. PARP12, an interferon-stimulated gene involved in the control of protein translation and inflammation. J Biol Chem **2014**;289:26642-57
148. Ashburner M, Ball CA, Blake JA, Botstein D, Butler H, Cherry JM, *et al.* Gene ontology: tool for the unification of biology. The Gene Ontology Consortium. Nat Genet **2000**;25:25-9
149. Brown GR, Hem V, Katz KS, Ovetsky M, Wallin C, Ermolaeva O, *et al.* Gene: a gene-centered information resource at NCBI. Nucleic Acids Res **2015**;43:D36-42
150. Duvaud S, Gabella C, Lisacek F, Stockinger H, Ioannidis V, Durinx C. Expasy, the Swiss Bioinformatics Resource Portal, as designed by its users. Nucleic Acids Res **2021**;49:W216-W27
151. Sievers F, Higgins DG. Clustal omega. Curr Protoc Bioinformatics **2014**;48:3.13.1-6
152. Ye J, Coulouris G, Zaretskaya I, Cutcutache I, Rozen S, Madden TL. Primer-BLAST: a tool to design target-specific primers for polymerase chain reaction. BMC Bioinformatics **2012**;13:134
153. Rebay I, Fehon RG. Preparation of insoluble GST fusion proteins. Cold Spring Harb Protoc **2009**;2009:pdb.prot4997
154. Cencic R, Hall DR, Robert F, Du Y, Min J, Li L, *et al.* Reversing chemoresistance by small molecule inhibition of the translation initiation complex eIF4F. Proc Natl Acad Sci U S A **2011**;108:1046-51

155. Boussif O, Lezoualc'h F, Zanta MA, Mergny MD, Scherman D, Demeneix B, *et al.* A versatile vector for gene and oligonucleotide transfer into cells in culture and in vivo: polyethylenimine. Proc Natl Acad Sci U S A **1995**;92:7297-301
156. Kingston RE, Chen CA, Rose JK. Calcium phosphate transfection. Curr Protoc Mol Biol **2003**;Chapter 9:Unit 9.1
157. Stepinski J, Waddell C, Stolarski R, Darzynkiewicz E, Rhoads RE. Synthesis and properties of mRNAs containing the novel "anti-reverse" cap analogs 7-methyl(3'-O-methyl)GpppG and 7-methyl (3'-deoxy)GpppG. RNA **2001**;7:1486-95
158. Cencic R, Pelletier J. A cautionary note on the use of cap analogue affinity resins. Anal Biochem **2018**;560:24-9
159. Aken BL, Ayling S, Barrell D, Clarke L, Curwen V, Fairley S, *et al.* The Ensembl gene annotation system. Database **2016**;2016:baw093
160. Alexander J, Lim D, Joughin BA, Hegemann B, Hutchins JR, Ehrenberger T, *et al.* Spatial exclusivity combined with positive and negative selection of phosphorylation motifs is the basis for context-dependent mitotic signaling. Sci Signal **2011**;4:ra42
161. Fagerberg L, Hallström BM, Oksvold P, Kampf C, Djureinovic D, Odeberg J, *et al.* Analysis of the human tissue-specific expression by genome-wide integration of transcriptomics and antibody-based proteomics. Mol Cell Proteomics **2014**;13:397-406
162. Li S, Sonenberg N, Gingras AC, Peterson M, Avdulov S, Polunovsky VA, *et al.* Translational control of cell fate: availability of phosphorylation sites on translational repressor 4E-BP1 governs its proapoptotic potency. Mol Cell Biol **2002**;22:2853-61
163. Rapley J, Oshiro N, Ortiz-Vega S, Avruch J. The mechanism of insulin-stimulated 4E-BP protein binding to mammalian target of rapamycin (mTOR) complex 1 and its contribution to mTOR complex 1 signaling. J Biol Chem **2011**;286:38043-53
164. Li D, Gong B, Xu J, Ning B, Tong W. Impact of Sequencing Depth and Library Preparation on Toxicological Interpretation of RNA-Seq Data in a "Three-Sample" Scenario. Chem Res Toxicol **2021**;34:529-40
165. Dowell RD. The similarity of gene expression between human and mouse tissues. Genome Biol **2011**;12:101
166. Gu X, Su Z. Tissue-driven hypothesis of genomic evolution and sequence-expression correlations. Proc Natl Acad Sci U S A **2007**;104:2779-84
167. Uhlén M, Fagerberg L, Hallström BM, Lindskog C, Oksvold P, Mardinoglu A, *et al.* Proteomics. Tissue-based map of the human proteome. Science **2015**;347:1260419
168. Friday AJ, Keiper BD. Positive mRNA Translational Control in Germ Cells by Initiation Factor Selectivity. Biomed Res Int **2015**;2015:327963
169. Ciosk R, DePalma M, Priess JR. Translational regulators maintain totipotency in the Caenorhabditis elegans germline. Science **2006**;311:851-3
170. Henderson MA, Cronland E, Dunkelbarger S, Contreras V, Strome S, Keiper BD. A germline-specific isoform of eIF4E (IFE-1) is required for efficient translation of stored mRNAs and maturation of both oocytes and sperm. J Cell Sci **2009**;122:1529-39
171. Ghosh S, Lasko P. Loss-of-function analysis reveals distinct requirements of the translation initiation factors eIF4E, eIF4E-3, eIF4G and eIF4G2 in Drosophila spermatogenesis. PLoS One **2015**;10:e0122519
172. Buchan JR. mRNP granules. Assembly, function, and connections with disease. RNA Biol **2014**;11:1019-30

173. Huggins HP, Subash JS, Stoffel H, Henderson MA, Hoffman JL, Buckner DS, *et al.* Distinct roles of two eIF4E isoforms in the germline of Caenorhabditis elegans. J Cell Sci **2020**;133
174. Cencic R, Yan Y, Pelletier J. Homogenous time resolved fluorescence assay to identify modulators of cap-dependent translation initiation. Comb Chem High Throughput Screen **2007**;10:181-8
175. Zuberek J, Wyslouch-Cieszynska A, Niedzwiecka A, Dadlez M, Stepinski J, Augustyniak W, *et al.* Phosphorylation of eIF4E attenuates its interaction with mRNA 5' cap analogs by electrostatic repulsion: intein-mediated protein ligation strategy to obtain phosphorylated protein. RNA **2003**;9:52-61
176. Cheng L, Albers P, Berney DM, Feldman DR, Daugaard G, Gilligan T, *et al.* Testicular cancer. Nature Reviews Disease Primers **2018**;4:29
177. Daugaard G, Gundgaard MG, Mortensen MS, Agerbæk M, Holm NV, Rørth M, *et al.* Surveillance for stage I nonseminoma testicular cancer: outcomes and long-term follow-up in a population-based cohort. J Clin Oncol **2014**;32:3817-23
178. Cheng L, Davidson DD, Montironi R, Wang M, Lopez-Beltran A, Masterson TA, *et al.* Fluorescence In Situ Hybridization (FISH) Detection of Chromosomal 12p Anomalies in Testicular Germ Cell Tumors. Methods Mol Biol **2021**;2195:49-63
179. Taylor-Weiner A, Zack T, O'Donnell E, Guerriero JL, Bernard B, Reddy A, *et al.* Genomic evolution and chemoresistance in germ-cell tumours. Nature **2016**;540:114-8
180. Romano FJ, Rossetti S, Conteduca V, Schepisi G, Cavaliere C, Di Franco R, *et al.* Role of DNA repair machinery and p53 in the testicular germ cell cancer: a review. Oncotarget **2016**;7:85641-9
181. Loveday C, Litchfield K, Proszek PZ, Cornish AJ, Santo F, Levy M, *et al.* Genomic landscape of platinum resistant and sensitive testicular cancers. Nature Communications **2020**;11:2189
182. Zhou C, Zhao X-m, Li X-f, Wang C, Zhang X-t, Liu X-z, *et al.* Curcumin inhibits AP-2γ-induced apoptosis in the human malignant testicular germ cells in vitro. Acta Pharmacol Sin **2013**;34:1192-200
183. Tomczak K, Czerwińska P, Wiznerowicz M. The Cancer Genome Atlas (TCGA): an immeasurable source of knowledge. Contemp Oncol (Pozn) **2015**;19:A68-77
184. Halliday GC, O'Reilly J, Kelsey C, Cole CH, Kotecha RS. Successful Treatment of Congenital Erythroleukemia With Low-Dose Cytosine Arabinoside. Pediatr Blood Cancer **2016**;63:566-7
185. Huret J-L. t (1; 8)(p22-p32; q22-q23). Atlas of Genetics and Cytogenetics in Oncology and Haematology **2009**
186. Rabkin CS, Janz S. Mechanisms and consequences of chromosomal translocation. Cancer epidemiology, biomarkers & prevention : a publication of the American Association for Cancer Research, cosponsored by the American Society of Preventive Oncology **2008**;17:1849-51